


1-1-2013

The Anti-Angiogenic Effects of Sparstolonin B

Henry Rhodes Bateman
University of South Carolina

Follow this and additional works at: <https://scholarcommons.sc.edu/etd>

 Part of the [Biomedical Commons](#), and the [Chemicals and Drugs Commons](#)

Recommended Citation

Bateman, H. R. (2013). *The Anti-Angiogenic Effects of Sparstolonin B*. (Doctoral dissertation). Retrieved from <https://scholarcommons.sc.edu/etd/2090>

This Open Access Dissertation is brought to you by Scholar Commons. It has been accepted for inclusion in Theses and Dissertations by an authorized administrator of Scholar Commons. For more information, please contact dillarda@mailbox.sc.edu.

THE ANTI-ANGIOGENIC EFFECTS OF SPARSTOLONIN B

by

Henry Rhodes Bateman, III

Bachelor of Science
Virginia Polytechnic Institute and State University, 2000

Master of Science
Virginia Commonwealth University, 2003

Submitted in Partial Fulfillment of the Requirements

For the Degree of Doctor of Philosophy in

Biomedical Science

School of Medicine

University of South Carolina

2013

Accepted by:

Susan M. Lessner, Major Professor

Daping Fan, Chairman, Examining Committee

Francis G. Spinale, Committee Member

Ugra S. Singh, Committee Member

Rekha C. Patel, Committee Member

Lacy Ford, Vice Provost and Dean of Graduate Studies

© Copyright by Henry Bateman, 2013
All Rights Reserved.

DEDICATION

I would like to dedicate this work to my family. My family has been extremely supportive and helpful during my completion of this program. My parents have always been devoted to my siblings and me, sacrificing everything to help us realize our dreams. My mother, who passed away seven years ago, was the greatest teacher in my life. Her love and support helped guide me to where I am today. She dedicated her life to her children. I always admired her optimism and desire to help everyone. Like my mother, my father has been an amazing role model and a caring and supportive parent. He is always there for advice and provides the best answers to any question that I may have. I am also inspired by my father's perseverance and courage. I would also like to acknowledge my twin brother, Ropon, and three sisters, Irma, Amy, and Julia. I have a strong bond with all my siblings; we have always striven to help each other. Throughout my life, I have viewed them as my role models. I am also thankful for my nieces and nephews. They always know how to brighten my day. I am so grateful to be part of such a loving family. I know my mother would be proud of all of us today.

ACKNOWLEDGEMENTS

I would like to acknowledge Dr. Susan M. Lessner for serving as my advisor and allowing me to become a part of her laboratory in the Department of Cell Biology and Anatomy. Dr. Lessner has been the best advisor in the world. I am very grateful that she accepted me into her lab in the summer of 2009. From the start, she has been an amazing advisor, mentor, and teacher. I have greatly appreciated and valued her support and encouragement. Her dedication to research and vast knowledge of biology and engineering is truly inspiring. She has helped me acquire the research, mentoring, and teaching skills necessary for me to excel in my future career in biomedical research.

I would also like to thank Dr. Daping Fan for initiating the Sparstolonin B project which would ultimately serve as the basis for my dissertation. Dr. Fan also served as the chairman of my graduate committee. He has been very helpful and supportive, and he has always been a great person to answer difficult questions.

I would like to acknowledge my committee members, Dr. Rekha Patel, Dr. Frank Spinale, and Dr. Ugra Singh. I am honored to have each one of them on my committee, and I would like to thank them for their encouragement, advice, and support. They provided me with direction and great ideas on how to proceed with my research project. I would also like to thank Dr. Kevin Carnevale for previously serving on my committee.

In addition, I would like to thank everyone from Dr. Lessner's lab (past and present), including John Johnson, Shana Watson, Ying Wang, Nishant Karasala,

Mohamed Gabr, Marwa Belhaj, and Lindsey Davis, for their encouragement and support. They helped make the lab a fun and enjoyable place to work. Furthermore, I am thankful for their assistance with my research project. I would also like to thank my student assistants, including Vanessa Rodriguez, Gabrielle Jenkins, Jeanny Nguyen, Rett Haney, and Melanie Gerhardt. Not only did these high school and undergraduate students assist me greatly with my research, but they also gave me the opportunity to serve as a teacher, something I would like to pursue in the future.

I would also like to thank Dr. Jay Potts, Na Li, and Keith Moore for assisting me with the CAM assay and RT-PCR. Dr. Jay Potts helped me start the initial CAM assay experiments, and he provided invaluable advice. I would like to acknowledge Dr. Richard Goodwin and Ashleigh Riley for providing eggs for the CAM assay and for technical assistance and advice. In addition, I would like to thank Dr. Udai Singh for helping me with the flow cytometry experiments, and I would like to thank Dr. Jeremy Barth and Dr. Scott Argraves for the large role they played in the microarray experiments.

ABSTRACT

Sparstolonin B (SsnB) is a novel bioreactive compound isolated from *Sparganium stoloniferum*, an herb historically used in Traditional Chinese Medicine as an anti-tumor agent. SsnB has demonstrated anti-inflammatory properties, inhibiting Toll-like receptor mediated inflammation in isolated macrophages and in mice. Angiogenesis, the process of new capillary formation from existing blood vessels, is dysregulated in many pathological disorders, including atherosclerosis, diabetic retinopathy, and tumor growth. The goal of the project was to investigate the anti-angiogenic effects of SsnB.

The first part of the project utilized *in vitro* functional assays to study how SsnB affected endothelial cells. SsnB inhibited endothelial cell tube formation (Matrigel method) and cell migration (Transwell method) in a dose-dependent manner. Microarray experiments with human umbilical vein endothelial cells (HUVECs) and human coronary artery endothelial cells (HCAECs) demonstrated differential expression of several hundred genes in response to SsnB exposure (916 and 356 genes, respectively, with fold change ≥ 2 , $p < 0.05$, unpaired t-test). Microarray data from both cell types showed significant overlap, including genes associated with cell proliferation and cell cycle. Flow cytometric cell cycle analysis of HUVECs treated with SsnB showed an increase of cells in the G1 phase and a decrease of cells in the S phase. Cyclin E2 (CCNE2) and Cell division cycle 6 (CDC6) are regulatory proteins that control cell cycle progression through the G1/S checkpoint. Both CCNE2 and CDC6 were downregulated in the

microarray data. Real Time quantitative PCR confirmed that gene expression of CCNE2 and CDC6 in HUVECs was downregulated after SsnB exposure, to 64% and 35% of controls, respectively. The data suggest that SsnB may exert its anti-angiogenic properties by downregulating CCNE2 and CDC6, halting progression through the G1/S checkpoint.

In the second portion of the project, a chick chorioallantoic membrane (CAM) assay was utilized to investigate SsnB inhibition of *ex vivo* angiogenesis. Chick embryos were exposed to methylcellulose discs containing vehicle control (DMSO) or SsnB. Chick embryos receiving SsnB discs showed significant reduction in capillary length and branching relative to the vehicle control group. Overall, SsnB caused a significant reduction in angiogenesis, demonstrating its *ex vivo* efficacy.

TABLE OF CONTENTS

DEDICATION	iii
ACKNOWLEDGEMENTS.....	iv
ABSTRACT	vi
LIST OF TABLES	x
LIST OF FIGURES	xi
LIST OF ABBREVIATIONS.....	xii
CHAPTER 1: INTRODUCTION.....	1
CHAPTER 2: SPARSTOLONIN B INHIBITS PRO-ANGIOGENIC FUNCTIONS AND BLOCKS CELL CYCLE PROGRESSION IN ENDOTHELIAL CELLS.....	17
2.1 ABSTRACT	17
2.2 INTRODUCTION.....	18
2.3 EXPERIMENTAL PROCEDURES	20
2.4 RESULTS.....	25
2.5 DISCUSSION.....	31
CHAPTER 3: THE UTILIZATION OF THE CHICK CHORIOALLANTOIC MEMBRANE ASSAY TO EXAMINE THE <i>EX VIVO</i> ANTI-ANGIOGENIC EFFECTS OF SPARSTOLONIN B.....	36
3.1 ABSTRACT	36
3.2 INTRODUCTION.....	37
3.3 EXPERIMENTAL PROCEDURES	43

3.4 RESULTS	45
3.5 DISCUSSION	48
CHAPTER 4: DISCUSSION.....	54
REFERENCES	72
APPENDIX A – SUPPLEMENTARY DATA	79

LIST OF TABLES

Table 2.1 Comparison of RT-PCR and Microarray Results	31
Table A.1 Gene function enrichment analysis for HUVECs in response to SsnB treatment.....	79
Table A.2 Gene function enrichment analysis for HCAECs in response to SsnB treatment.....	81

LIST OF FIGURES

Figure 1.1 Atherosclerotic Plaque Progression.....	2
Figure 1.2 Structure of SsnB.....	11
Figure 1.3 Cell Cycle	12
Figure 2.1 SsnB inhibits endothelial cell tube formation on Matrigel.....	26
Figure 2.2 SsnB inhibits endothelial cell migration.....	27
Figure 2.3 SsnB arrests endothelial cells in the G1 phase of the cell cycle.....	29
Figure 3.1 Chick embryo demonstrating chorioallantoic membrane vascularization	41
Figure 3.2 SsnB reduces normalized blood vessel length in the CAM assay.....	46
Figure 3.3 SsnB reduces normalized branch number in the CAM assay.....	47
Figure 3.4 Representative images from CAM assay	48
Figure A.1 8-Isoprostane Staining in Sections of Carotid Arteries	84
Figure A.2 SsnB inhibits Matrigel tube formation in HMVECs	85
Figure A.3 Heatmap of differentially regulated genes in HUVECs and HCAECs	86
Figure A.4 Heatmap of differentially regulated genes in HUVECs and HCAECs	87
Figure A.5 SsnB causes G2/M blockage in non-synchronized HUVECs	88
Figure A.6 Representative images demonstrating double nuclei.....	88

LIST OF ABBREVIATIONS

8-IP	8-Isoprostane
AHR	Aryl Hydrocarbon Receptor
ALDH3A1	Aldehyde Dehydrogenase 3 Family, Member A1
ANLN	Anillin
ARNT	AHR Nuclear Translocator
AURKA	Aurora Kinase A
AURKB	Aurora Kinase B
bFGF	Basic Fibroblast Growth Factor
CAM	Chorioallantoic Membrane
CAV1	Caveolin-1
CCNB1	Cyclin B1
CCNE2	Cyclin E2
CDC2	Cell Dependent Kinase 1
CDC6	Cell Division Cycle 6
DIAPH3	Diaphanous Homolog 3
DMSO	Dimethyl Sulfoxide
ECM	Extracellular Matrix
FBS	Fetal Bovine Serum
GAPDH	Glyceraldehyde-3-Phosphate Dehydrogenase
HCAEC	Human Coronary Artery Endothelial Cells
HIF	Hypoxia Inducible Factor

HMMR	Hyaluronan-Mediated Motility Receptor
HMVEC	Human Microvascular Endothelial Cells
HUVEC.....	Human Umbilical Vein Endothelial Cells
KIF18A	Kinesin Family Member 18A
KITLG.....	KIT Ligand
MAPK.....	Mitogen-Activated Protein Kinase
MMP	Matrix Metalloproteinase
NF- κ B	Nuclear Factor-Kappa B
NO.....	Nitric Oxide
PA	Plasminogen Activator
RHAMM.....	Hyaluronan-Mediated Motility Receptor
ROS.....	Reactive Oxygen Species
SsnB	Sparstolonin B
TACC3.....	Transforming Acidic Coiled-Coil Containing Protein 3
TCM.....	Traditional Chinese Medicine
TLR.....	Toll-like Receptor
VC.....	Vehicle Control
VEGF	Vascular Endothelial Growth Factor

CHAPTER 1

INTRODUCTION

Atherosclerosis

Atherosclerosis is a serious chronic disease affecting a significant portion of the U.S. population and causing many deaths, from conditions such as ischemic stroke and myocardial infarction. There are many risk factors for atherosclerosis including hypertension, smoking, diabetes, high-fat diet, and dyslipidemia. Atherosclerosis specifically involves the formation of plaques within blood vessels, progressing through several stages (illustrated in Figure 1.1). In the earliest stage, fatty streaks or atheromas form as lipids and lipoproteins deposit in the tunica intima of the blood vessel. A high ratio of LDL:HDL favors this event. The lipid deposits become oxidized and induce injury to the endothelial cells lining the blood vessel. Endothelial injury is a key step in atherosclerosis; endothelial cells may also be injured by denuding events or by more subtle hemodynamic changes. Cell adhesion molecules are upregulated in the endothelium, and inflammatory cells are attracted to the site of injury, including monocytes which differentiate into macrophages. As macrophages migrate to the area of oxidized lipids, scavenger receptors and toll-like receptors bind the lipids and help activate the macrophages to release inflammatory cytokines and mediators. The macrophages transform into foam cells as they take up oxidized lipids. Additional cells migrate to the area, including mast cells and leukocytes. An advanced lesion forms as

smooth muscle cells from the tunica media proliferate, migrate into the plaque, and form a fibrous cap. The smooth muscle cells may also transform into foam cells. An area of dead cells and cholesterol crystals forms within the plaque. A capillary network also grows within the plaque to help provide nutrients, gases, and inflammatory cells to the growing plaque. Blood vessels within the tunica adventitia, known as the vasa vasorum, supply this capillary network. As the plaque progresses, the fibrous cap weakens and ruptures, exposing the highly thrombogenic necrotic core region. Thrombus formation subsequently ensues. The thrombus may occlude the vessel or become an embolus that travels to another region of the body (Sluimer and Daemen 2009).

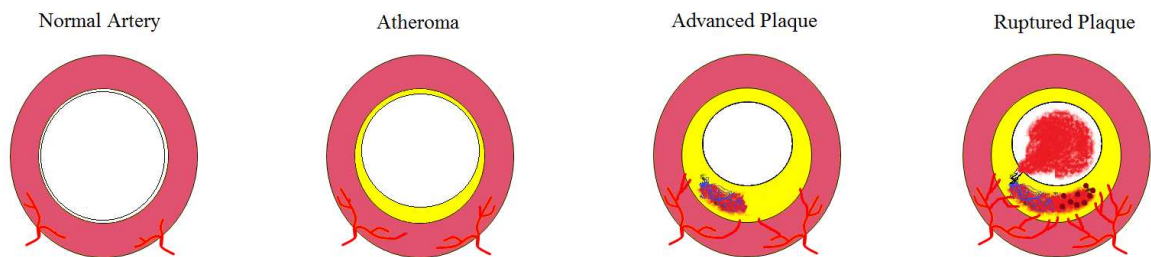


Figure 1.1 Atherosclerotic Plaque Progression.

Plaque formation does not typically occur in wild type mice. However, ApoE knockout mice and LDL receptor knockout mice show significant plaque progression after several months on a high fat diet (such as the Western Diet). Plaque formation in mice can be accelerated by surgical interventions which alter hemodynamics or induce endothelial injury. These procedures include complete and partial carotid ligation, where the entire common carotid artery or its branches are ligated with sutures. The resulting decreased blood flow and oscillatory shear stress reduce the time to plaque formation. Another model of atherosclerosis in mice is wire-induced endothelial cell injury. In this

model, a wire is inserted into the carotid artery, and the luminal surface is scraped to induce endothelial injury. A similar model involves the application of electrical current to the carotid. Mice may also be injected with lipopolysaccharide, derived from gram negative bacteria, to induce an inflammatory response and cause atherosclerosis (Nam et al. 2009).

Intraplaque Angiogenesis

Atherosclerotic plaque rupture is the leading cause of acute cardiovascular events such as myocardial infarction (“heart attack”) and ischemic stroke. In this process, the fibrous cap overlying an atherosclerotic plaque fails, resulting in rapid thrombus formation which may completely occlude the vessel, leading to ischemia and tissue death downstream of the blockage. Newly developed and recurring myocardial infarction afflicts approximately 1.1 million people in the USA per year, with a 40% fatality rate; 220,000 of these deaths occur without hospitalization. Roughly 75% of these clinical events are caused by atherosclerotic plaque rupture. Clearly, methods of stabilizing atherosclerotic plaques to prevent plaque rupture would have a significant clinical impact (Sluimer and Daemen 2009).

Research has shown a link between capillary networks within atherosclerotic plaques and plaque progression and rupture (Sluimer et al. 2009). Under normal physiological conditions, only thick-walled blood vessels such as the descending aorta and the common carotid artery contain an intramural capillary network. This network of blood vessels, known as the vasa vasorum, is situated in the tunica adventitia and outer third of the tunica media. It supplies the blood vessel wall with nutrients and allows gas

exchange. Human atherosclerotic arteries have shown extensive intraplaque angiogenesis, often linked to the vasa vasorum. It has been suggested that hypoxia and/or reactive oxygen species are responsible for initiating new capillary formation (Khurana et al. 2005). Capillary networks within atherosclerotic plaques serve as a source of inflammatory cells, nutrients, and mediators, allowing the neo-intima to expand beyond the normal wall thickness. Intraplaque angiogenesis is correlated with decreased plaque stability and increased incidence of plaque rupture, subsequent thrombus formation, and intra-arterial occlusion. Recent research has suggested that inhibiting angiogenesis may improve plaque stability and decrease the chances for plaque rupture (Moreno et al. 2004; Virmani et al. 2005). In addition, inhibiting angiogenesis may decrease plaque formation by limiting this supply of necessary factors to the plaque region (Sluimer and Daemen 2009).

Oxidative stress and reactive oxygen species (ROS) have been linked to many different pathological states, including atherosclerosis. ROS are also employed in normal physiological responses in vascular cells, including intracellular signaling. ROS include hydrogen peroxide, superoxide anion, nitric oxide (NO), peroxynitrite, and hydroxyl radical. Sources of ROS include NADPH oxidases, eNOS, lipoxygenases, the mitochondrial electron chain, and xanthine oxidase. Reactive oxygen species can also be found in environmental sources, such as cigarette smoke and diesel exhaust fumes. Certain reactive oxygen species, such as the superoxide anion, may react with NO, forming peroxynitrite which oxidizes and damages lipid membranes, lipoproteins, and cellular enzymes. As NO becomes inactivated, vasodilation is impaired, resulting in a state of hypertension. ROS may also increase cell adhesion molecules in endothelial

cells, leading to a state of vascular inflammation. All of the preceding effects predispose the vasculature to atherosclerosis (Ushio-Fukai et al. 1999).

Steps Involved in Angiogenesis

Angiogenesis is one mechanism of new blood vessel formation. Specifically, angiogenesis refers to capillary formation from existing blood vessels; whereas, vasculogenesis refers to the *de novo* formation of blood vessels during embryogenesis. Angiogenesis plays an important role in many normal events in the body, including wound healing, embryogenesis, and female reproductive processes. During these normal processes, angiogenesis is highly regulated. Unregulated angiogenesis contributes to many pathological conditions, such as rheumatoid arthritis, psoriasis, retinopathy, and tumor growth and metastasis. Clearly, angiogenesis is an important event in the human body. In addition, endothelial cells play a key role during angiogenesis. Therefore, an understanding of endothelial cell functions is essential when discussing angiogenesis (Bussolino, Mantovani, and Persico 1997).

Angiogenesis is a complex event that occurs in several stages and involves interactions between cells, soluble factors, and extracellular matrix molecules. First, proteolytic enzymes break down the basement membrane of an existing blood vessel. Endothelial cells with the help of proteolytic enzymes, including matrix metalloproteinases (MMPs) and the plasminogen activator system (PA), break down the basement membrane and invade the surrounding tissues. The PA system is comprised of the serine proteases urokinase-type plasminogen activator (uPA) and tissue-type plasminogen activator (tPA) that convert plasminogen into its active form, plasmin.

Plasmin degrades numerous extracellular matrix proteins, including fibronectin, laminin, and fibrin. Plasmin also helps activate many MMPs. Matrix metalloproteinases are more specific in the matrix molecules that they degrade. After the basement membrane of the blood vessel is broken down, endothelial cells migrate into the surrounding tissue and proliferate. Growth factors and other soluble proteins in the ECM often facilitate and regulate this process. The growth factors that are stored bound to the ECM can be released as the ECM is degraded by proteases. Certain growth factors, such as vascular endothelial growth factor, act as chemoattractants that facilitate the migration of endothelial cells to certain locations. After proliferation and migration, the endothelial cells form a new lumen and start to secrete extracellular matrix molecules, ultimately forming a new capillary (Liekens, De Clercq, and Neyts 2001).

Preliminary Research

The strong connection between plaque instability and angiogenesis initially captured our attention. What causes intraplaque angiogenesis? How can we inhibit intraplaque angiogenesis? Will inhibiting angiogenesis prevent plaque rupture? These were questions that first intrigued us. Our preliminary research sought to investigate the cause and process of angiogenesis within atherosclerotic plaques. We hypothesized that reactive oxygen species were responsible for capillary formation within plaques. Later we decided to investigate the anti-angiogenic properties of the plant derived compound Sparstolonin B. We will first begin with a brief description of the preliminary research conducted on reactive oxygen species and intraplaque angiogenesis. The majority of this dissertation will then be devoted to examining Sparstolonin B and its anti-angiogenic properties.

To study the relationship between reactive oxygen species, angiogenesis, and atherosclerosis, a mouse model of atherosclerosis was utilized. In this model, ApoE knockout mice underwent left carotid ligation. The ligated mice were placed on a high cholesterol diet (Paigen Diet - 1.25% cholesterol) for 0, 7, 14, and 21 days. During this time, atherosclerotic plaques developed within each ligated carotid artery. After the appropriate time course, the mice were sacrificed and perfused with heparinized saline and neutral buffered formalin. Both left and right carotid arteries were dissected in an entire block, including the trachea and esophagus. Carotid blocks were fixed, processed, and embedded in paraffin. The specimens were sectioned into 5 um sections and collected on glass slides. Plaque formation was demonstrated by hematoxylin and eosin (H&E) and Masson's Trichrome staining. To investigate reactive oxygen species formation in the plaque, antibodies against 8-isoprostane (8-IP) were chosen. 8-IP forms after reactive oxygen species react with components of the cell membrane. The slides were deparaffinized and hydrated; immunohistochemical staining was performed to detect 8-IP. A colorimetric reaction was utilized to detect the presence of 8-IP. Light microscopic images were acquired with a 10X objective lens, and the stained area within sections was measured with Image-Pro Plus image analysis software.

Immunohistochemical staining for 8-IP was performed on carotid artery sections taken from mice that had undergone a complete carotid artery ligation for 0, 7, 14, or 21 days. The staining results were analyzed by dividing each carotid image into three separate regions (intima, media, and adventitia) and measuring the positively stained area in each region (see Appendix, Figure A.1). The media region exhibited the least amount of staining in all sections; whereas, the adventitia exhibited the most staining. Day 14

specimens demonstrated the largest stained area, and Day 0 showed the least staining. Overall, 8-IP seemed to increase over time and peak on Day 14. Afterwards, 8-IP staining dropped on Day 21. In addition, Day 14 and 21 sections showed areas of 8-IP staining that overlapped with capillary networks identified by antibody Ter 119 (erythroid cell marker) and hematoxylin and eosin stains. Day 7, 14, and 21 sections exhibited 8-IP staining in areas containing foam cells and adventitial fat cells. Day 0 staining was confined to the endothelium. These results suggest that ROS formation increases during atherosclerotic plaque development in this mouse model.

The results demonstrated a potential role for reactive oxygen species in capillary formation within atherosclerotic plaques. 8-isoprostane is formed when reactive oxygen species react with arachidonic acid, a component of cellular membranes. Since 8-IP is elevated in the neointima at 14 and 21 days after carotid ligation, this implies that reactive oxygen species are present in the atherosclerotic plaques. The colocalization of 8-IP and intraplaque capillary networks suggests that ROS may be involved in neovascularization. Day 14 sections demonstrate 8-IP staining before intraplaque vessels are present, supporting this hypothesis. Hypoxia has been shown to be a major driving force for angiogenesis, but other factors, such as reactive oxygen species, may play a key role in this process. ROS may activate many of the same angiogenic pathways as hypoxia, including the stabilization of the transcription factor hypoxia inducible factor (HIF)-1 α which upregulates VEGF. Future directions could incorporate research into the mechanisms of ROS stimulation of angiogenesis and additional markers of ROS, such as 4-hydroxynonenal (4-HNE).

Angiogenesis Inhibition and Sparstolonin B

The research outlined above explored a potential stimulus for intraplaque angiogenesis. After completing this research, it was deemed important to investigate new ways to inhibit angiogenesis. New methods to inhibit angiogenesis may hold the key to new treatments not only for atherosclerosis, but also for various other angiogenesis-related pathological conditions, including psoriasis, cancer, and rheumatoid arthritis. Sparstolonin B (SsnB) is a newly isolated compound from the aquatic herb, *Sparganium stoloniferum*. Based on prior research conducted on both SsnB and the parent plant (described in the following pages), we hypothesized that SsnB would inhibit angiogenesis.

Angiogenesis may be inhibited at multiple steps. Growth factors, including Vascular Endothelial Growth Factor (VEGF) and basic Fibroblast Growth Factor (bFGF), are suitable targets. Current approaches to sequester VEGF include soluble VEGF receptors and neutralizing antibodies against VEGF. Intracellular signaling molecules, including tyrosine kinases, can be inhibited to prevent receptor-mediated activation of endothelial cells. There also exist natural angiogenesis inhibitors, including endostatin, retinoids, and fibronectin fragment, which may be targeted for angiogenesis inhibition. Angiogenesis inhibitors often target endothelial cells through the inhibition of cell proliferation, migration, and protease production. Current research into angiogenesis inhibition has demonstrated ways to limit atherosclerosis. By inhibiting intraplaque angiogenesis, necessary factors, such as inflammatory cells, oxygen, and mediators, are not delivered to the growing plaque, diminishing plaque growth. Plaque stability may

also be improved, decreasing the likelihood of plaque rupture and subsequent thrombosis and stroke or myocardial infarction (Pandya, Dhalla, and Santani 2006).

Sparstolonin B (SsnB) is a novel bioactive compound isolated from the plant *Sparganium stoloniferum* by Dr. Qiaoli Liang from the laboratory of Dr. Daping Fan at the University of South Carolina School of Medicine (Liang et al. 2011). *Sparganium stoloniferum* is a perennial, aquatic plant grown in North and East China, whose tubers have long been used in Traditional Chinese Medicine (TCM) for the treatment of several inflammatory diseases and as an anti-spasmodic and anti-tumor agent. Previous work with this herb has mainly dealt with its extracts. SsnB is one of several chemical compounds that have been isolated and characterized from *Sparganium stoloniferum*. NMR and X-ray crystallography have identified SsnB as a polyphenol with structural similarities to isocoumarins and xanthone (see Figure 1.2). Isocoumarins are a class of compounds that often exhibit anti-coagulant, anti-inflammatory, and anti-tumor properties (Qiu 2008; Liang et al. 2011; Xiong et al. 2009).

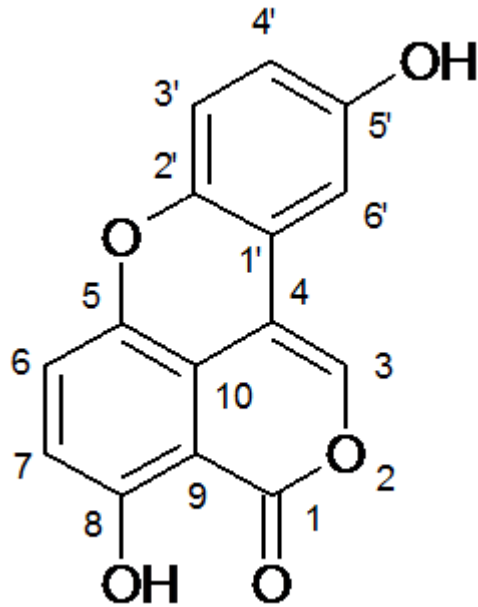


Figure 1.2 Structure of SsnB

SsnB shows potential as a safe, non-toxic pharmaceutical agent for the treatment of several pathological conditions. At concentrations up to 100 μM , SsnB does not exhibit cytotoxic effects on various cell types, including peritoneal mouse macrophages, phorbol myristate acetate (PMA)-differentiated THP-1 macrophages, Human Umbilical Vein Endothelial Cells (HUVECs), Human Aortic Smooth Muscle Cells (HASMCs), and monocytic THP-1 cells. Prior research has shown that SsnB exhibits strong anti-inflammatory effects on mouse and human macrophages, selectively inhibiting the inflammatory responses of macrophages to ligands for Toll-like Receptors 2 and 4 (TLR2 and TLR4). SsnB has also been shown to suppress downstream signaling pathways after TLR2 and TLR4 activation, including MAPK and NF- κB . These findings suggest that SsnB may be an antagonist to TLR2 and TLR4 (Liang et al. 2011).

Targeting endothelial cell proliferation has shown potential in the area of angiogenesis inhibition. Endothelial cell proliferation may be inhibited in numerous ways, including the downregulation of cell cycle regulatory proteins (Pandya, Dhalla, and Santani 2006). Cyclins and cyclin dependent kinases are regulatory proteins that control progression through the cell cycle by regulating specific cell cycle checkpoints. Cyclins help activate cyclin dependent kinases, which phosphorylate downstream proteins that allow cells to progress through these checkpoints. Cyclin E2 (CCNE2) and Cell Division Cycle 6 (CDC6) are regulatory proteins that control progression through the G1 checkpoint (see Figure 1.3). Downregulation of CCNE2 and CDC6 could trap cells at the G1 checkpoint and prevent endothelial cells from entering the final stages of cell division (Wu et al. 2009; Borlado and Mendez 2008). We have hypothesized that SsnB may exert anti-angiogenic effects by downregulating CCNE2 and CDC6, trapping endothelial cells at the G1 checkpoint and preventing complete cell division.

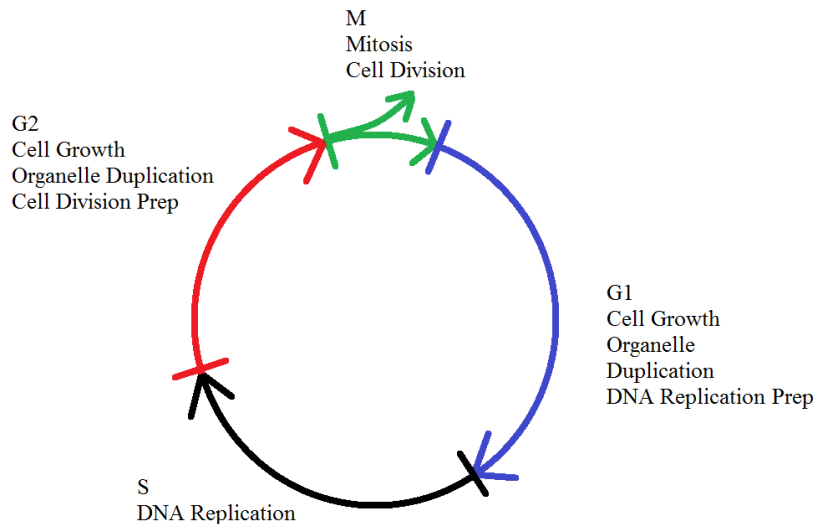


Figure 1.3 Cell Cycle

The parent plant *Sparganium stoloniferum* has been used for centuries in Traditional Chinese Medicine for the treatment of cancer. Furthermore, previously published research has shown that extracts and other isolated chemical compounds from this herb, including a sucrose ester, a phenylpropanoid glycerol, carboxylic acid esters, and a phenylpropanoid glycoside, have demonstrated potent anti-cancer effects (Li et al.). Compounds used to treat tumors often possess the ability to inhibit angiogenesis, among other properties. This enables these compounds to limit blood vessel growth into growing tumors, limiting the supply of necessary nutrients and cells and subsequently inhibiting tumor growth (Meng et al.). Since SsnB is derived from this plant used in cancer treatment, we tested the hypothesis that SsnB may possess anti-angiogenic properties in addition to its already established anti-inflammatory properties. Moreover, SsnB offers advantages over current protein angiogenesis inhibitors, including angiostatin and thrombospondin, which require parenteral administration.

Specific Aims

The overall goal of the project is to demonstrate that SsnB inhibits angiogenesis and to determine its mechanism of action in blocking angiogenesis. Our initial *in vitro* studies demonstrated the potential of SsnB as an anti-angiogenic agent, which inhibits human endothelial cell tube formation and migration. Our microarray data showed how SsnB affected gene expression, with an enrichment of differentially regulated genes associated with cell proliferation, replication, migration, and cell cycle. SsnB arrested endothelial cell division in the G1 phase in association with downregulating the cell cycle proteins cdc6 and cyclin E2. Furthermore, we demonstrated that SsnB inhibited *ex vivo* angiogenesis in the chick chorioallantoic membrane assay. Overall, we hypothesize that

SsnB inhibits angiogenesis by targeting endothelial cell cycle progression, cell migration, and chemotaxis. The project may ultimately demonstrate the potential of SsnB as a pharmaceutical compound used to inhibit angiogenesis and possibly to stabilize atherosclerotic plaques.

Specific Aim 1 – Functional Assays:

To demonstrate the anti-angiogenic effects of SsnB through *in vitro* functional assays using human endothelial cells.

Specific Aim 2 – Mechanistic Studies:

A. Microarray:

To test the effects of SsnB on the gene expression profile of Human Umbilical Vein Endothelial Cells (HUVECs) and Human Coronary Artery Endothelial Cells (HCAECs).

B. Cell Cycle Regulation:

To investigate how SsnB affects expression of genes for cell cycle regulatory proteins and progression through the cell cycle.

Specific Aim 3 – *Ex vivo* Studies:

To demonstrate the anti-angiogenic effects of SsnB in the *ex vivo* chick chorioallantoic membrane (CAM) assay.

Specific Aim 1 involved the use of several *in vitro* functional assays to reveal if and how SsnB inhibited angiogenesis-related functions in isolated endothelial cells.

Specific Aim 2 further investigated the mechanism of inhibition by examining changes in gene expression with microarrays and determining how SsnB affected cell cycle progression. Specific Aim 3 demonstrated angiogenesis inhibition in an *ex vivo* system.

Overall, SsnB exhibits many diverse effects, including anti-inflammatory, anti-

angiogenic, and cytostatic properties, which suggest that it may have potential therapeutic uses for a plethora of disorders.

.

CHAPTER 2

SPARSTOLONIN B INHIBITS PRO-ANGIOGENIC FUNCTIONS AND BLOCKS CELL CYCLE PROGRESSION IN ENDOTHELIAL CELLS

Abstract

Sparstolonin B (SsnB) is a novel bioactive compound isolated from *Sparganium stoloniferum*, an herb historically used in Traditional Chinese Medicine as an anti-tumor agent. Angiogenesis, the process of new capillary formation from existing blood vessels, is dysregulated in many pathological disorders, including diabetic retinopathy, tumor growth, and atherosclerosis. In functional assays, SsnB inhibited endothelial cell tube formation (Matrigel method) and cell migration (Transwell method) in a dose-dependent manner. Microarray experiments with human umbilical vein endothelial cells (HUVECs) and human coronary artery endothelial cells (HCAECs) demonstrated differential expression of several hundred genes in response to SsnB exposure (916 and 356 genes, respectively, with fold change ≥ 2 , $p < 0.05$, unpaired t-test). Microarray data from both cell types showed significant overlap, including genes associated with cell proliferation and cell cycle. Flow cytometric cell cycle analysis of HUVECs treated with SsnB showed an increase of cells in the G1 phase and a decrease of cells in the S phase. Cyclin E2 (CCNE2) and Cell division cycle 6 (CDC6) are regulatory proteins that control cell cycle progression through the G1/S checkpoint. Both CCNE2 and CDC6 were downregulated in the microarray data. Real Time quantitative PCR confirmed that gene expression of CCNE2 and CDC6 in HUVECs was downregulated after SsnB exposure, to

64% and 35% of controls, respectively. The data suggest that SsnB may exert its anti-angiogenic properties in part by downregulating CCNE2 and CDC6, halting progression through the G1/S checkpoint.

Introduction

Sparstolonin B (SsnB) is a novel bioactive compound isolated from the plant *Sparganium stoloniferum*, a perennial, aquatic plant grown in North and East China, whose tubers have long been used in Traditional Chinese Medicine (TCM) for the treatment of several inflammatory diseases and as an anti-spasmodic and anti-tumor agent. NMR and X-ray crystallography have identified SsnB as a polyphenol with structural similarities to isocoumarins, a class of compounds that often exhibit anti-coagulant, anti-inflammatory, and anti-tumor properties (Qiu 2008; Xiong et al. 2009; Liang et al. 2011). SsnB may hold potential as a safe, non-toxic pharmaceutical agent for the treatment of several pathological conditions. At concentrations up to 100 μ M, SsnB does not exhibit cytotoxic effects on various cell types, including mouse peritoneal macrophages, HUVECs, human aortic smooth muscle cells, and monocytic THP-1 cells. Prior research has shown that SsnB exhibits strong anti-inflammatory effects on mouse and human macrophages by selectively inhibiting the inflammatory responses of macrophages to ligands for Toll-like Receptor (TLR) 2 and TLR4. SsnB has also been shown to suppress downstream signaling pathways after TLR2 and TLR4 activation, including MAPK and NF- κ B (Liang et al. 2011). These findings suggest that SsnB may be an antagonist to TLR2 and TLR4.

Angiogenesis refers to capillary formation from existing blood vessels.

Angiogenesis plays an important role in many physiological events in the body, including

wound healing, embryogenesis, and female reproductive processes (Folkman 1971; Risau 1997). During these normal processes, angiogenesis is highly regulated. Unregulated, excessive angiogenesis contributes to many pathologies, such as rheumatoid arthritis, psoriasis, retinopathy, and tumor growth and metastasis (Staton, Reed, and Brown 2009). Inhibiting pathological angiogenesis may prove to be an effective therapy for these angiogenesis-related diseases.

Angiogenesis is a complex process that occurs in several stages and involves interactions between cells, soluble factors, and extracellular matrix molecules. Endothelial cells play a key role in angiogenesis. Endothelial cells can secrete proteolytic enzymes which break down the basement membrane of an existing blood vessel, allowing the cells to invade the surrounding tissues, migrate in response to an angiogenic stimulus, and proliferate. Growth factors and other soluble proteins in the ECM often facilitate and regulate this process, including vascular endothelial growth factor (VEGF). The endothelial cells form a new lumen, start to secrete extracellular matrix molecules, and ultimately form a new capillary (Bussolino, Mantovani, and Persico 1997; Carmeliet 2003; Liekens, De Clercq, and Neyts 2001). Mural cells are also recruited to the site and play an important role in angiogenesis. Angiogenesis may be inhibited at any of these key steps (Pandya, Dhalla, and Santani 2006). Targeting endothelial cell proliferation, cell migration, and chemotaxis have shown potential in angiogenesis inhibition.

In the present study, we demonstrate that SsnB inhibits endothelial cell functions related to angiogenesis in several *in vitro* functional assays. The data suggests the potential of SsnB as an anti-angiogenic agent by showing inhibition of human endothelial cell tube formation and migration. We have also examined the effects of SsnB on

endothelial cell gene expression, focusing in particular on pathways related to angiogenesis. In addition, our data show that SsnB arrests endothelial cell division in the G1 phase and downregulates the cell cycle proteins cdc6 and cyclin E2. Overall, these findings add anti-angiogenic and cytostatic properties to the list of diverse effects exhibited by SsnB.

Experimental Procedures

Materials – Sparstolonin B was purified from the plant *Sparganium stoloniferum* according to previously published methods (Liang et al. 2011). The purity of SsnB was determined to be greater than 99% by HPLC, and a stability test was utilized to ensure that samples were consistently > 99% pure.

Cell Culture - Human coronary artery endothelial cells (HCAECs), human umbilical vein endothelial cells (HUVECs), and human cardiac microvascular endothelial cells (HMVECs) were obtained from Lonza (Hopkinton, MA) and cultured on polystyrene, tissue culture-treated petri plates (100 X 20 mm) coated with 0.1% gelatin. HUVECs, HCAECs, and HMVECs were cultured in endothelial cell medium supplemented with 10% fetal bovine serum (FBS) and endothelial cell mitogen / growth supplement (Biomedical Technologies, Stoughton, MA). The endothelial cell medium was replaced every 2-3 days, and the cells were passaged after complete confluence was reached. Confluent plates were trypsinized and split, and the cells were cultured until the fourth passage was reached.

Matrigel Tube Formation Assay - To initially determine if SsnB inhibited pro-angiogenic cell functions, a tube formation assay with Matrigel was performed. Growth factor reduced Matrigel (BD Biosciences, Bedford, MA) was added to the wells of a 96

well polystyrene culture plate and incubated at 37 °C for 30 minutes. Cells (HUVECs, HCAECs, or HMVECs at passage 2 to 4) were added to each well to reach a final number of 20,000 cells per well. SsnB was added to the wells at a concentration of 1, 10, or 100 μ M. Endothelial cell medium with DMSO (0.1%) was used as a vehicle control. Each group contained 4 replicates. The plates were placed in an incubator for 4 h. During the incubation, the endothelial cells formed elongated structures called cords, also known as tubes. After 4 h, neutral buffered formalin was added to fix the cells. Pictures of three non-overlapping fields were taken from each well. The lengths of single cell endothelial cords were measured with Image-Pro Plus (Media Cybernetics, Silver Spring, MD), and the sum of tube lengths for each well was determined. The average total length and standard deviation for each group were determined, and the appropriate statistical tests (ANOVA and Newman-Keuls) were completed. The tube formation assay was replicated three times for both HUVECs and HCAECs. The assay was also repeated with cardiac HMVECs.

Cell Viability - A Live/Dead assay (Invitrogen, Eugene, OR) was utilized to investigate the effect of SsnB on cell viability. The Matrigel tube formation experiment was repeated with HUVECs in chamber slides at a concentration of 20,000 cells per well. The cells were treated with SsnB (1, 10, or 100 μ M) or Vehicle Control (0.1% DMSO) as described above. After four hours of incubation, the slides were removed. A chamber slide containing HUVECs treated with 70% methanol for 30 minutes was used as a control for dead cell staining. The slides were aspirated and washed with PBS, and EthD-1 and calcein AM were added to each well. The plates were incubated in the dark, and images were taken with a light microscope at 10X magnification..

Transwell Insert Cell Migration Assay - The cell invasion assay was performed with a Transwell insert system (6.5 mm diameter inserts with 8.0 μm pores in a polycarbonate membrane situated in wells of 24 well polystyrene, tissue culture treated plates, Corning Incorporated, Corning, NY). The Transwell inserts were coated with 0.1% gelatin for 30 min and incubated in low serum medium for 1 h. Cultured HUVECs were trypsinized and then resuspended in low serum medium (0.5% fetal bovine serum without endothelial cell mitogen), and added at 50,000 cells per insert. The cells were allowed to adhere to the inserts for 30 min. Next, various concentrations of SsnB (0.0001, 0.001, 0.01, 0.1, 1, 10, and 100 μM) or vehicle control (0.1% DMSO) were added to the Transwell inserts. After 30 min, the medium in the lower chamber for the experimental groups was replaced with low serum medium containing 10 ng/ml VEGF, establishing a chemoattractant gradient between the top insert and lower chamber. For the negative control group, the medium was replaced with low serum medium (0.5% fetal bovine serum). The plates were incubated for 8 h at 37°C. During the incubation, the cells migrated through the pores of the Transwell insert towards the lower chamber. At the end of this period, cells on the upper surface of the insert were removed, and migrated cells on the bottom side were fixed in formalin and stained with Hoechst dye (a fluorescent nuclear stain). The filter inserts were removed from the wells and mounted on glass slides. Cells were counted from four random fields observed with a 10X objective lens. The cell migration experiments were repeated three times at high SsnB concentrations (0.1, 1, 10, 100 μM) and one time at low SsnB concentrations (0.0001, 0.001, 0.01, 0.1 μM) for HUVECs.

Cell Cycle Analysis - Cell cycle analysis was performed using propidium iodide staining and flow cytometry. HUVECs (approximately 75% confluent) cultured in 6 well polystyrene culture plates coated with 0.1% gelatin were serum starved for 24 hours in low serum medium containing 0.5% fetal bovine serum and no endothelial cell mitogen to synchronize the cells in the G0/G1 phase. After 24 hours, the low serum medium was replaced with treatments of either 100 μ M SsnB or vehicle control (0.1% DMSO) diluted in complete growth medium (10% fetal bovine serum with endothelial cell mitogen) in triplicate. The treated cells were incubated for 24, 30, and 36 hours. After incubation, the cells were trypsinized, transferred to 5 ml polystyrene round bottom tubes (12 X 75 mm), and centrifuged. The medium was aspirated, and the cells were washed with PBS. After fixing the cells with ice-cold 70% ethanol for 15 min, the cells were centrifuged and stained with propidium iodide for 30 min. The samples were then analyzed with a flow cytometer (Beckman Coulter FC500). The unstained and stained cell groups were used to calibrate the settings on the flow cytometer. The data were collected and analyzed with ModFit software.

Microarray Analysis - Confluent plates (100 X 20 mm polystyrene, tissue culture-treated petri plates coated with 0.1% gelatin, 75% confluent) of HUVECs and HCAECs (four plates for HUVECs, n=2, and six plates for HCAECs, n=3) were chosen for the microarray experiments. Half of the plates received complete growth medium (10% fetal bovine serum with endothelial mitogen) containing vehicle control (0.1% DMSO), and the remaining plates received complete growth medium containing 100 μ M SsnB. The plates were incubated for 24 h to allow SsnB to have an effect on cellular gene expression. Following incubation, RNA isolation was completed with the RNeasy Mini

kit from Qiagen. The cells were lysed, and RNA was isolated by using the RNeasy spin columns and following the protocol provided by Qiagen. Purified RNA was sent to the Medical University of South Carolina Proteogenomics Facility for microarray analysis. The GeneChip Human Genome U133 Plus 2.0 Array was utilized to track changes in gene expression due to SsnB treatment. Complete data was uploaded to the NCBI Gene Expression Omnibus database (accession number GSE44598).

Real Time RT-PCR - After a careful analysis of the microarray data, key genes (CDC6, CCNE2, KITLG, ALDH3A1, CCNB1, CDC2, HMMR, DIAPH3, ANLN, and CDKN3) were chosen for quantitative real-time PCR (qRT-PCR) to verify the gene expression results. HCAECs and HUVECs were exposed to SsnB or vehicle control for 24 h (as previously described in the microarray section). For RT-PCR, RNA was isolated from the cells with the RNeasy Mini kit as described previously. After forward and reverse primer kits (Qiagen, Valencia, CA) were selected, the RNA was amplified. The one-step RT-PCR reactions were completed on the BioRad iCycler thermal cycler system in the Instrumentation Resource Facility at the USC School of Medicine. The expression levels were normalized, and RNA levels were quantified.

Data Analysis - Microarray data analysis, including data normalization (robust multi-array average), identification of differentially expressed genes (comparative analyses with dChip software), and heat map construction, was carried out to determine how SsnB affects gene expression and affected pathways (n = 2 for HUVECs and n = 3 for HCAECs). After a careful analysis of the microarray data, several key genes were chosen for qRT-PCR to verify the gene expression results. The genes were chosen based on the following criteria: fold change ≥ 2 , $p < 0.05$, unpaired t-test with a false discovery

rate approximating 0%, appearing in both data sets (HUVECs and HCAECs), and gene function relating to cell proliferation and/or angiogenesis. For qRT-PCR, the expression levels were normalized to the housekeeping gene GAPDH, and RNA levels were compared between groups with the $\Delta\Delta C_t$ method.

Results

SsnB inhibits endothelial cell tube formation and cell migration - Figures 2.1 and 2.2 show representative results from the tube formation and cell migration assays with HUVECs. SsnB treatment resulted in a dose-dependent inhibition of HUVEC tube formation at concentrations between 1 and 100 μM ($p < 0.05$, Newman-Keuls test). SsnB also demonstrated a dose-dependent inhibition of VEGF-induced cell migration at concentrations between 0.0001 and 0.1 μM ($p < 0.05$), which leveled off between 0.1 and 100 μM ($p < 0.05$). Experiments with HCAECs also demonstrated a dose-dependent inhibition (between 1 and 100 μM) of endothelial cell tube formation on the substrate Matrigel (Figure 2.1). A dose-dependent inhibition of tube formation was also seen with cardiac HMVECs (see Appendix, Figure A.2). Results from the live/dead assay with HUVECs showed that SsnB had no effect on cell viability at the concentrations used. Cells treated with SsnB or vehicle control showed positive staining for live cells, but no staining for dead cells (red fluorescence). These data suggest that SsnB is able to inhibit endothelial cell morphogenesis and that cell migration, a crucial process in angiogenesis, may play a role.

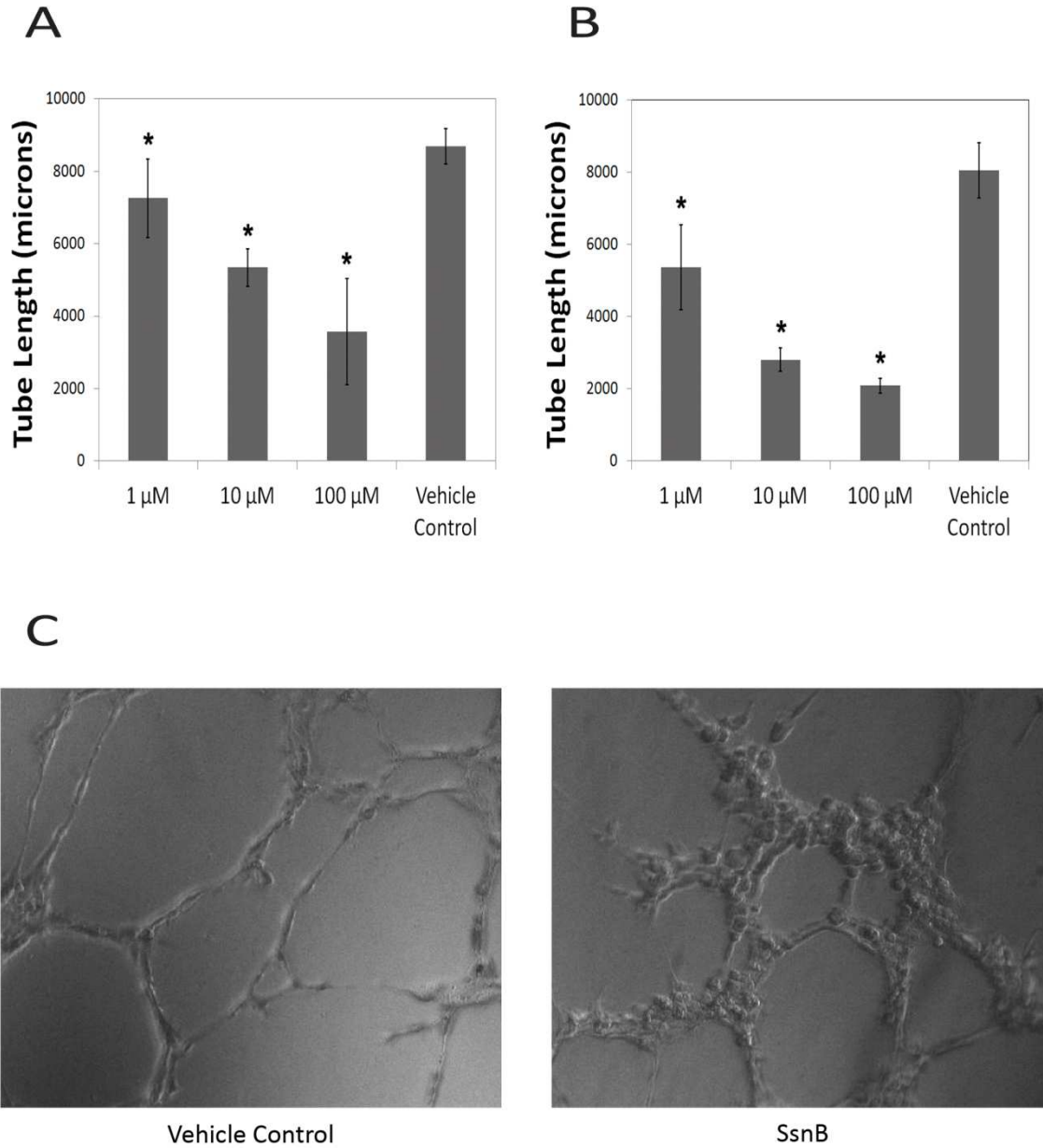


Figure 2.1 SsnB inhibits endothelial cell tube formation on Matrigel. A. Total tube length as a function of SsnB concentration in HUVECs. B. Total tube length as a function of SsnB concentration in HCAECs. * $p < 0.05$ vs. vehicle control, Newman-Keuls test. C. Representative micrographs demonstrating tube formation in HUVECs (left – vehicle control, right – 100 μ M SsnB).

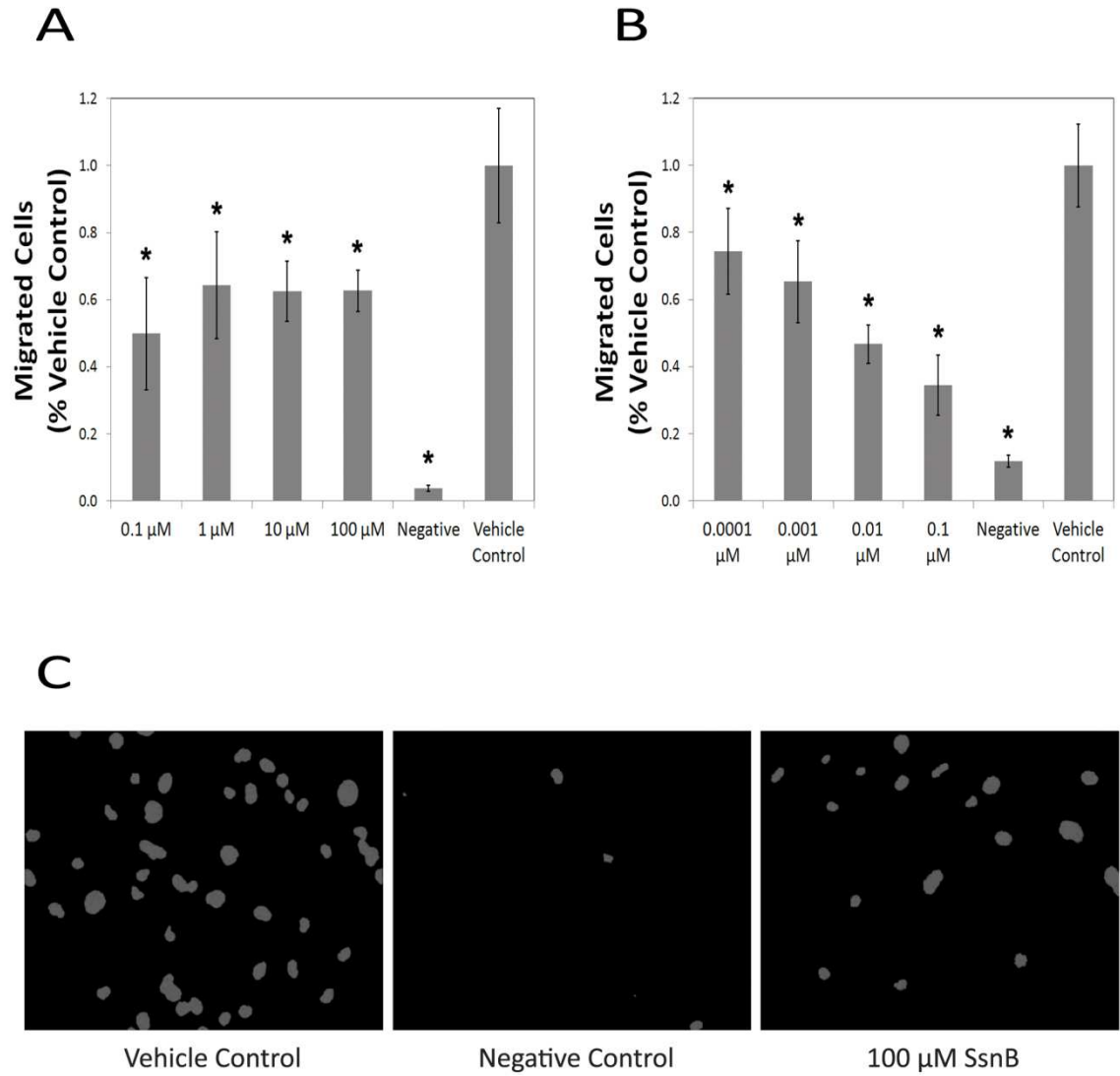
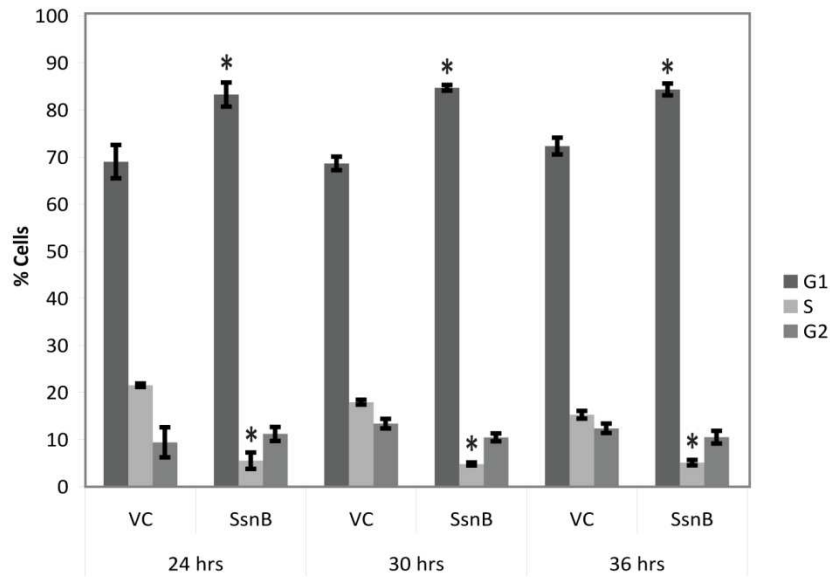


Figure 2.2 SsnB inhibits endothelial cell migration. A. Migrated cells as a function of SsnB concentration (0.1 to 100 μM). B. Migrated cells as a function of SsnB concentration (0.0001 to 0.1 μM) shows a dose-dependent response. * $p < 0.05$ vs. vehicle control, Newman-Keuls test. C. Representative micrographs demonstrating cell migration (left – vehicle control, center – negative control, right – 100 μM SsnB).

SsnB arrests endothelial cells in the G1 phase of the cell cycle - Figure 2.3 depicts representative results from the cell cycle experiments. In comparison to vehicle controls, flow cytometric cell cycle analysis of HUVECs treated with SsnB showed an increase of cells in the G1 phase and a decrease of cells in the S phase after 24, 30, and 36 hours of treatment. In untreated cells, the percentage of cells in S phase decreased and the percentage in G2/M increased from 24 to 36 hours after addition of growth medium, as expected once cells begin to re-enter and move through the cell cycle. Overall, these results imply that endothelial cells are being arrested in the G0/G1 phase, suggesting an inhibition of cell proliferation, an important step in angiogenesis.

A



B

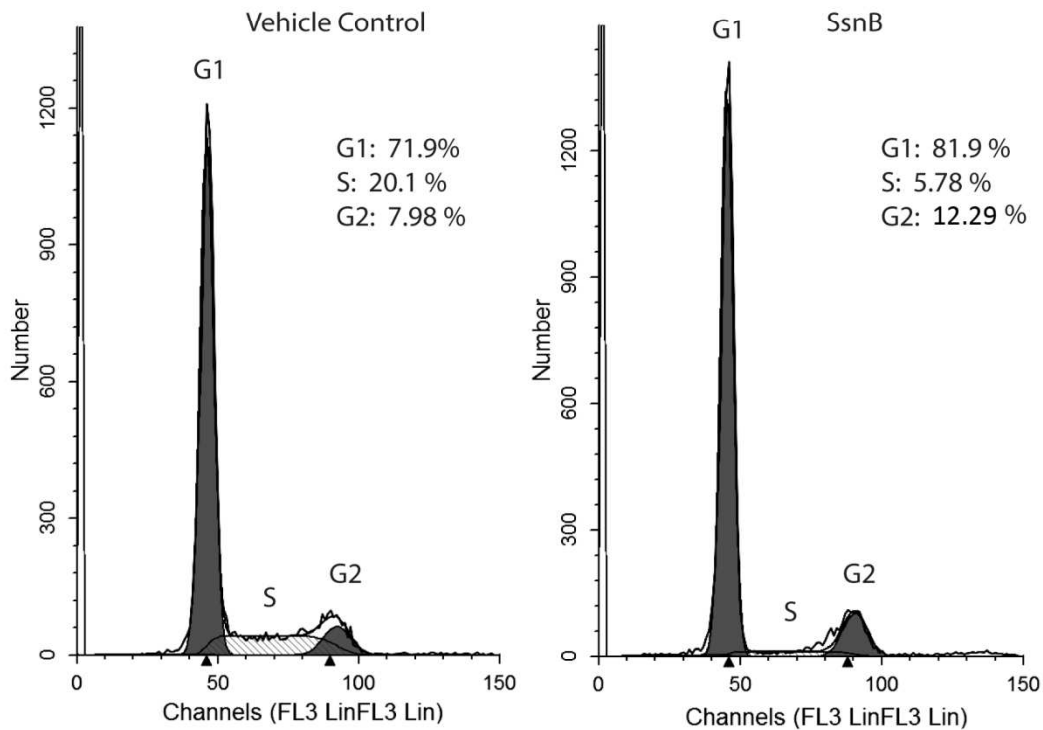


Figure 2.3 SsnB arrests endothelial cells in the G1 phase of the cell cycle. A. After 24, 30, and 36 hours of treatment, 100 μ M SsnB decreased the percentage of cells in the S phase and increased the percentage of cells in the G1 phase. * $p < 0.005$ vs. corresponding vehicle control, Newman-Keuls test. B. Representative cell cycle data demonstrating the increase in G1 cell percentage and decrease in S phase cell percentage after 24 hours of SsnB treatment (left - vehicle control, right - SsnB)

SsnB changes the expression of genes associated with cell cycle and cell proliferation - Microarray experiments demonstrated differential expression of several hundred genes in response to SsnB exposure (916 genes for HUVECs and 356 genes for HCAECs, fold change ≥ 2 , $p < 0.05$, unpaired t-test with a false discovery rate approximating 0%). Supplementary Table A.1 and Supplementary Table A.2 present the results of the gene function enrichment analysis for HUVECs and HCAECs, respectively. Overall, microarray data from both cell types showed significant overlap, including genes in pathways associated with cell proliferation, cytoskeleton, chemotaxis, and cell cycle, all areas implicated in angiogenesis. These results are consistent with the data obtained from the cell migration and cell cycle functional studies. From this microarray study, it is clear that SsnB regulates genes involved in angiogenic processes in HUVECs and HCAECs.

Real Time RT-PCR - Following microarray data analysis, key genes (listed in Table 2.1) were chosen for verification with real time RT-PCR. Cyclin E2 (CCNE2) and Cell division cycle 6 (CDC6) are regulatory proteins that control cell cycle progression through the G1/S checkpoint. Both CCNE2 and CDC6 were downregulated in the microarray data. qRT-PCR confirmed that gene expression of CCNE2 and CDC6 was downregulated after SsnB exposure to 64% and 35% of controls respectively for HUVECs and to 57% and 14% of controls respectively for HCAECs. Kit-Ligand (KITLG), also known as stem cell factor, is a protein involved in the differentiation and growth of stem cells. Aldehyde dehydrogenase 3 family, member A1 (ALDH3A1) is a protein involved in the aryl hydrocarbon receptor pathway. These genes were chosen for further study because they were highly upregulated by SsnB treatment in the microarray

data set. In HUVECs, qRT-PCR analysis demonstrated that KITLG and ALDH3A1 expression was upregulated to 400% and 1280% of controls, respectively. In HCAECs, KITLG and ALDH3A1 expression was upregulated to 260% and 4620% of controls, respectively. The microarray data was supported in both data sets.

Table 2.1 Comparison of RT-PCR and Microarray Results. Fold expression change vs. vehicle control.

Gene	HUVECs			HCAECs		
	PCR $2^{\Delta\Delta Ct}$ value	Microarray		PCR $2^{\Delta\Delta Ct}$ value	Microarray	
		Fold change value	p-value		Fold change value	p-value
KITLG	4.0	6.2	0.02795	2.6	2.1	0.00010
ALDH3A1	12.8	7.7	0.00609	46.2	8.8	0.00001
HMMR	0.24	0.11	0.03073	0.062	0.20	0.00006
DIAPH3	0.19	0.34	0.03248	0.26	0.38	0.00019
ANLN	0.20	0.09	0.00900	0.13	0.11	0.000001
CDKN3	0.18	0.19	0.01471	0.22	0.18	0.00018
CCNB1	0.40	0.19	0.02304	0.13	0.16	0.00003
CDC2	0.14	0.08	0.00440	0.17	0.20	0.00004
CDC6	0.35	0.23	0.01527	0.14	0.18	0.00185
CCNE2	0.64	0.24	0.01814	0.57	0.38	0.00180

Discussion

Pathological angiogenesis is associated with many disorders, including rheumatoid arthritis, diabetic retinopathy, and psoriasis. Recent research has shown that inhibiting angiogenesis may prove to be an effective therapeutic option in treating these disorders. In the present study, potential anti-angiogenic effects of SsnB were demonstrated in several *in vitro* functional assays with endothelial cells, including the Matrigel tube formation assay and the Transwell insert cell migration assay. SsnB was

also shown to arrest endothelial cells in the G1 phase of the cell cycle. The cellular functions tested in these assays represent key steps in angiogenesis that are inhibited by SsnB, including cell proliferation, cell migration, and chemotaxis. To further investigate the mechanism of action for SsnB, we utilized microarray analysis to examine how SsnB affected gene expression in endothelial cells. After SsnB exposure, genes associated with cell proliferation, cell cycle, chemotaxis, and the cytoskeleton were differentially regulated in both HUVECs and HCAECs. Our data suggest that SsnB alters gene expression in these pro-angiogenic pathways.

Targeting endothelial cell proliferation has shown potential in the area of angiogenesis inhibition. Endothelial cell proliferation may be inhibited in numerous ways, including the downregulation of cell cycle regulatory proteins (Pandya, Dhalla, and Santani 2006). Cyclins and cyclin dependent kinases are regulatory proteins that control progression through the cell cycle by regulating specific cell cycle checkpoints. Cyclins help activate cyclin dependent kinases, which phosphorylate downstream proteins that allow cells to progress through these checkpoints. Cyclin E2 (CCNE2) and Cell division cycle 6 (CDC6) are regulatory proteins that control progression through the G1/S checkpoint. CDC6 regulates DNA replication, and cyclin E2 activates cyclin-dependent kinase 2 (Wu et al. 2009; Borlado and Mendez 2008). Downregulation of CCNE2 and CDC6 will trap cells at the G1/S checkpoint and prevent endothelial cells from initiating DNA replication. The cell cycle regulatory proteins, Cyclin E2 (CCNE2) and Cell division cycle 6 (CDC6), were both downregulated by SsnB treatment. Overall, our data suggest that SsnB downregulates the cell cycle regulatory proteins CCNE2 and CDC6, potentially trapping cells in the G1 phase and hindering cell proliferation, an important

step in angiogenesis (Nigg 2001; Sullivan and Morgan 2007; Tassan et al. 1994; O'Farrell 2001).

Our data shows that SsnB affects the gene expression of additional cell cycle regulatory proteins, including cyclin B1 (CCNB1) and cyclin dependent kinase 1 (CDC2). CCNB1 and CDC2 are regulatory proteins that control progression through the G2/M checkpoint. Downregulation of CCNB1 and CDC2 will trap cells at the G2/M checkpoint and prevent endothelial cells from entering the final stages of cell division. Table 2.1 demonstrates that CCNB1 and CDC2 were both downregulated by SsnB. In addition to preventing cell progression through the G1/S checkpoint, SsnB may also prevent progression through the G2/M checkpoint by downregulating these additional cell cycle proteins (Nigg 2001; Sullivan and Morgan 2007; Tassan et al. 1994; O'Farrell 2001). This effect is less readily seen due to blockage at the G1/S checkpoint.

Sparganium stoloniferum has long been used in Traditional Chinese Medicine for the treatment of cancer and seizures. Major chemical components from the stem and rhizome, including flavonoids, saponins, and phenylpropanoids, are responsible for these therapeutic effects (Li et al.). Anti-tumor agents often exhibit anti-angiogenic effects, among other cancer suppressing properties. Inhibiting angiogenesis cuts tumors off from the vasculature, limiting growth and metastasis (Meng et al.). Previously published research has shown that extracts derived from *Sparganium stoloniferum* have demonstrated potent anti-cancer effects. Isolated chemical compounds from this herb, including a sucrose ester, a phenylpropanoid glycerol, carboxylic acid esters, and a phenylpropanoid glycoside, demonstrated anti-tumor activities (Xiong et al. 2009; Lee et al.). In addition, the polyphenolic structure of SsnB also reveals much about its potential

therapeutic effects. Many plant-derived polyphenols have demonstrated anti-inflammatory and anti-angiogenic properties. Quercetin and resveratrol, both polyphenols isolated from red wine, have demonstrated anti-inflammatory and anti-angiogenic properties. In addition, oleuropein and hydroxytyrosol, both derived from virgin olive oil, reduce angiogenesis by inhibiting matrix metalloproteinase-9 (MMP-9) and cyclooxygenase-2 (COX-2) (Scoditti et al. 2012). Emodin, another plant-derived polyphenol similar to SsnB, has also been shown to inhibit angiogenesis by targeting endothelial cell proliferation (Kwak et al. 2006). Emodin causes a downregulation of CCNB1 and CDC2 and a cell cycle arrest at the G2/M phase (Wang, Wu, and Zhen 2004).

In addition to its effects on the cell cycle and cell proliferation, SsnB also affects other key steps of angiogenesis, including cell migration and chemotaxis. The microarray data for both HUVECs and HCAECs demonstrates an enrichment of genes associated with both pathways, including diaphanous homolog 3 (DIAPH3), hyaluronan-mediated motility receptor (HMMR), and anillin (ANLN), an actin binding protein. Furthermore, it is also important to investigate potential upstream pathways that lead to the alterations in gene expression seen in the microarray data. Previously published data have shown that SsnB can suppress the NF- κ B pathway, and prior studies have demonstrated a link between NF- κ B signaling and expression of cell cycle proteins. Genes for these regulatory proteins, such as CCNE2, CDC6, CCNB1, and CDC2, contain binding sites for NF- κ B (Hsu, Lee, and Pan; Cude et al. 2007; Liu et al. 2009; Wang et al.; Meteoglu et al. 2008). SsnB may suppress the NF- κ B pathway and cause a subsequent downregulation of the cell cycle regulatory proteins CCNE2 and CDC6.

SsnB has also been shown to inhibit the MAPK pathways, including JNK, ERK, and p38 signaling, which all affect gene expression and cell proliferation. We need to explore these relationships as potential mechanisms of angiogenesis inhibition.

Our current study with HUVECs and HCAECs demonstrates that SsnB inhibits angiogenic processes in functional assays, including the Matrigel tube assay, Transwell insert cell migration assay, and microarray analysis. Our next step is to demonstrate the *in vivo / ex vivo* efficacy of SsnB, to further evaluate its potential as an anti-angiogenic agent.

CHAPTER 3

THE UTILIZATION OF THE CHICK CHORIOALLANTOIC MEMBRANE ASSAY TO EXAMINE THE *EX VIVO* ANTI-ANGIOGENIC EFFECTS OF SPARSTOLONIN B.

Abstract

Pathological angiogenesis plays a significant role in many disorders, including atherosclerosis, diabetic retinopathy, and cancer. Inhibiting angiogenesis may offer a potential treatment for angiogenesis-dependent disorders. Sparstolonin B (SsnB), a novel bioactive compound isolated from *Sparganium stoloniferum*, has demonstrated the ability to inhibit pro-angiogenic functions in endothelial cells. In functional assays, SsnB inhibited endothelial cell tube formation (Matrigel method) and cell migration (Transwell method) in a dose-dependent manner. Microarray experiments with human umbilical vein endothelial cells (HUVECs) and human coronary artery endothelial cells (HCAECs) demonstrated differential expression of genes associated with cell proliferation and cell cycle. SsnB may exert its anti-angiogenic properties by downregulating CCNE2 and CDC6, halting progression through the G1/S checkpoint. To investigate the effects of SsnB on *ex vivo* angiogenesis, a chick chorioallantoic membrane (CAM) assay was utilized. Chick embryos were exposed to methylcellulose discs containing vehicle control (DMSO) or 100 micromolar SsnB. Chick embryos receiving SsnB discs showed significant reduction in capillary length and branching number relative to the vehicle control group. Overall, SsnB caused a significant reduction in angiogenesis, demonstrating its *ex vivo* efficacy.

Introduction

Angiogenesis refers to capillary formation from existing blood vessels; it is a complex process that occurs in several stages and involves interactions between cells, soluble factors, and extracellular matrix molecules. Endothelial cells play a key role in angiogenesis. First, proteolytic enzymes break down the basement membrane of an existing blood vessel and endothelial cells invade the surrounding tissues, migrate, and proliferate. Growth factors and other soluble proteins in the ECM, including Vascular Endothelial Growth Factor (VEGF), facilitate and regulate this process. After migration and proliferation, the endothelial cells form a new lumen and start to secrete extracellular matrix molecules, ultimately forming a new capillary. Supporting cells, such as pericytes and smooth muscle cells, and extracellular matrix proteins are also extensively involved in the process (Bussolino, Mantovani, and Persico 1997; Carmeliet 2003; Liekens, De Clercq, and Neyts 2001).

Angiogenesis plays an important role in many normal physiological functions and numerous pathological conditions. Physiological processes include embryonic development, wound healing, and changes in the endometrial wall. Pathological processes that involve angiogenesis include atherosclerosis, psoriasis, rheumatoid arthritis, and tumor growth and metastasis. Targeting angiogenesis may provide a potential therapy for these pathological disorders. Angiogenesis may be inhibited at multiple steps. Growth factors, including Vascular Endothelial Growth Factor and basic Fibroblast Growth Factor, are a suitable target. Current approaches to sequester VEGF include soluble VEGF receptors and neutralizing antibodies against VEGF. Intracellular signaling molecules, including tyrosine kinases, can be inhibited to prevent receptor-

mediated activation of endothelial cells. There also exist natural angiogenesis inhibitors, including endostatin, retinoids, and fibronectin fragment, which may be targeted for angiogenesis inhibition. Angiogenesis inhibitors often target endothelial cells through the inhibition of cell proliferation, migration, and protease production (Pandya, Dhalla, and Santani 2006). Current research into angiogenesis inhibition has demonstrated ways to limit atherosclerosis. By inhibiting intraplaque angiogenesis, necessary factors, such as inflammatory cells and mediators, are not delivered to the growing plaque, diminishing plaque growth. Plaque stability may also improve, decreasing the likelihood of plaque rupture and subsequent thrombosis and stroke or myocardial infarction (Virmani et al. 2005; Moreno et al. 2004; Sridhar and Shepherd 2003).

Sparstolonin B (SsnB) is a novel compound isolated from the plant *Sparganium stoloniferum*, a perennial, aquatic plant grown in North and East China. Dried powder and extracts derived from *Sparganium stoloniferum* have been used for centuries in Chinese folk medicine for the treatment of inflammatory diseases, seizures, and blood stasis. These compounds are also widely used to treat gynecological problems, including amenorrhea and cancer, such as hysteromyoma. Most significantly, one such extract has shown the ability to inhibit angiogenesis and estrogen-mediated activities (Sun, Wang, and Wei 2011). Extracts containing active components are isolated from the root-like modified stem of the plant, known as the rhizome or tuber. A typical extraction protocol involves drying the rhizome and grounding it into a powder. The powder is mixed in boiling distilled water to produce an aqueous solution. Extracts may also be prepared with organic solvents, including ethanol, chloroform, and ethyl acetate. Extracts contain a multitude of active components including flavonoids, phenylpropanoid glycosides,

aromatic acids, and polyphenols (Wu et al. 2012). Sparstolonin B isolation was begun by soaking the powdered tuber in 85% ethanol overnight and extracting three times with the same solvent. The solvent was filtered and concentrated under vacuum, producing a residue, which was then dissolved in water and extracted with petrol, ethyl acetate, and n-butyl alcohol in sequential order. This extract was run through a silica gel column and eluted with petrol - ethyl acetate mixtures with increasing polarities. The end product was yellow needles containing SsnB (Liang et al. 2011).

The potential effects that SsnB may have on biological pathways may be revealed by its chemical structure. The structure of SsnB is very similar to isocoumarin or xanthone, both compounds known for anti-coagulant, anti-inflammatory, and anti-tumor properties. Furthermore, the polycyclic / polyphenolic structure is suggestive of the ability of SsnB to serve as an angiogenesis inhibitor (Liang et al. 2011). Polyphenolic compounds derived from plants, including olives and grapes, have been shown to have anti-oxidant, anti-inflammatory, cardioprotective, and anti-cancer properties.

Compounds derived from green tea and red wine, particularly quercetin and resveratrol, have both demonstrated angiogenesis inhibition (Scoditti et al. 2012). Similarly, we have shown the ability of SsnB to inhibit *in vitro* angiogenesis. In functional assays with endothelial cells (HUVECs, HCAECs, and HMVECs), SsnB has demonstrated the ability to inhibit key steps of angiogenesis, including morphogenesis, cell migration, chemotaxis, and cell cycle progression. Using microarrays, we have shown that SsnB altered gene expression in pathways associated with the cell cycle, cytoskeleton, and cytokinesis. Furthermore, published research has shown that SsnB blocks Toll-like

receptor 2 and Toll-like receptor 4 mediated inflammation in human and murine macrophages (Liang et al. 2011).

Preliminary research into angiogenesis inhibitors or stimulators often begins with simple *in vitro* assays using endothelial cells, such as the Matrigel tube formation assay or Transwell insert migration assay. However, these assays only study isolated functions of endothelial cells. Angiogenesis is a multicellular event that also incorporates interactions with extracellular components. In order to fully prove that a compound inhibits or stimulates angiogenesis, an *in vivo* or *ex vivo* assay must be utilized to address the complex, multicellular nature of angiogenesis. Several commonly used *in vivo* assays include the Matrigel plug, corneal angiogenesis, and hamster cheek pouch assays. The chick chorioallantoic membrane (CAM) assay is also widely used to study *ex vivo* angiogenesis. The assay is simple and reproducible, and it reveals more important information than *in vitro* assays (Auerbach et al. 2003). The CAM is used for gas and nutrient exchange in the chick embryo during development. Figure 3.1 illustrates the organization of a typical CAM. The allantois appears 3 days after incubation as an evagination from the endodermal hind gut. After spreading into the extraembryonic coelom, the allantoic vesicle enlarges rapidly. The mesodermal layers of the allantois and chorion fuse to form the chorioallantoic membrane. This double layer becomes highly vascularized as blood vessels develop. Within the CAM, single walled immature blood vessels develop first, eventually forming a capillary plexus around day 8. All vessels are connected to branches from the two main chorioallantoic arteries and one chorioallantoic vein. At day 18, the vascular system reaches its final organization. Located near the porous shell, the highly vascularized CAM allows exchange of oxygen

and carbon dioxide and serves as an area to store waste products, including urea and uric acid. The rapidly developing vascular system in the CAM provides an ideal environment to study how compounds affect angiogenesis (Ribatti 2008).

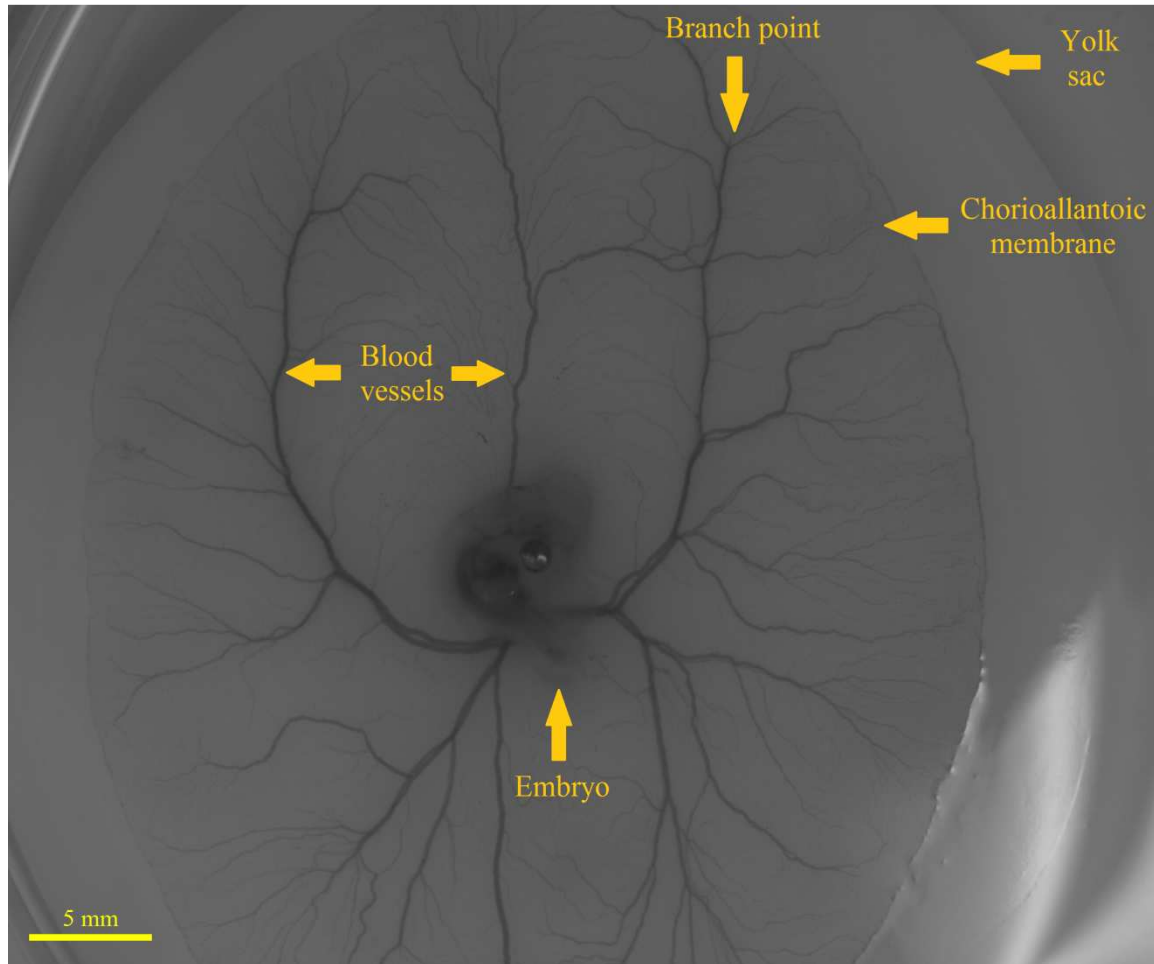


Figure 3.1 Chick embryo demonstrating chorioallantoic membrane vascularization.

In the CAM assay, test compounds are added to the surface of the CAM, and their effect on angiogenesis is examined. Delivery systems include synthetic polymer discs, gelatin sponges, or glass coverslips. One of the most popular methods involves the creation of discs made from a solution of 1% methylcellulose mixed with the test compound. Methylcellulose discs allow slow release and minimal adverse biological

reaction (Swiercz et al. 1999). This assay may be completed with or without the intact shell (*in ovo* and *ex ovo*, respectively). For the *in ovo* method, eggs are incubated for 7 to 9 days, and a square hole is cut in the shell after removing albumin with a fine needle. Through this window, the test compounds are added. The window is sealed, and eggs are placed back in an incubator for 2 or 3 days. The *in ovo* method maintains a more physiological environment, but provides a very limited area of the CAM with which to work. In the shell-less or *ex ovo* method, day 3-4 incubated eggs are carefully cracked open, and the egg contents are transferred to plastic petri plates. The plates are incubated for an additional 2 to 6 days. This is technically a whole-animal assay, even though it shares much in common with *in vitro* assays. The *ex ovo* method provides a large surface area of the CAM to place test substances and easily document with time lapse photography. However, a high mortality rate is often associated with the *ex ovo* method, sometimes reaching 50% dead after the first three days (Dohle et al. 2009; Ribatti 2008; Auerbach et al. 2003).

In both assays, the angiogenic response in the CAM may be measured in numerous ways. For analysis, pictures may be taken at the end of the experiment or over time to document the progression of blood vessel growth. However, time progression photos involve excessive handling of the embryos, which increases the embryonic mortality rate. Images from the area surrounding and underneath the test compound may be qualitatively scored on a numeric scale, such as 0 to 4, based on vascularization. Qualitative analysis is quick and reproducible, but it requires initial serial dilution assays with controls to establish the grading scale. Quantitative methods have proven more accurate and less prone to human error. Quantitative techniques include the measurement

of blood vessel number, length, and area. Another quantitative procedure involves counting the number of converging vessels with superimposed rings on the CAM image. To address blood vessel branching, the number of bifurcation points may be counted, or fractal pattern analysis may be utilized. In addition, the total blood vessel volume in the CAM may be measured by injecting thymidine or a colorimetric / fluorescent dye. Many of these quantitative techniques involve time consuming manual analysis of images, which can be overcome with automated analysis by computer software algorithms (Ribatti 2008; Blacher et al. 2001).

Our preliminary studies with HUVECs, HCAECs, and HMVECs have shown evidence of the anti-angiogenic effects of SsnB in the Matrigel tube assay and the Transwell insert cell migration assay. However, we must also demonstrate the *in vivo* or *ex vivo* efficacy of SsnB if we would like to further evaluate SsnB as a potential pharmaceutical agent. The *in vitro* assays alone are not sufficient in this regard. We demonstrated the *ex vivo* anti-angiogenic effects of SsnB with the chick chorioallantoic membrane (CAM) assay.

Experimental Procedures

Materials - Sparstolonin B was purified from the plant *Sparganium stoloniferum* according to previously published methods (Liang et al. 2011). Fresh fertilized bovine eggs were obtained from Clemson University and stored at 4°C for no longer than one week.

Methylcellulose Discs - Methylcellulose discs were created with a solution of 0.5% methylcellulose (diluted in sterile deionized water). A methylcellulose solution of

100 micromolar SsnB was made by adding 1.1 microliters of stock SsnB (93 mM) to 1 ml 0.5% methylcellulose. A vehicle control solution was created by adding 1 microliter of dimethyl sulfoxide (DMSO) to 1 ml 0.5% methylcellulose. Discs were created by placing 20 microliter droplets of SsnB or vehicle control solution onto polytetrafluoroethylene tape (to minimize adherence during drying) and allowed to dry under a laminar flow hood.

Chick Chorioallantoic Membrane Assay - The fertilized eggs were placed in a humidified egg incubator with forced air circulation at 37°C. The eggs were automatically rotated every three hours. After 4 days of incubation, the eggs were removed and cracked. Chick embryos with intact yolks were placed in 100 mm petri plates. Each petri plate was placed in a weigh boat containing 13 ml Moscona's buffer and covered with cellophane wrap with two holes for air circulation. The plates were placed in a water-jacketed incubator (37C, 5% CO₂) for 2 days. After 2 days of incubation, the methylcellulose discs containing either SsnB or vehicle control were placed on top of the CAM of each embryo in the right upper quadrant in an area near the allantoic vessels. After 2 additional days of incubation, the CAMs were examined and photographed with a dissecting stereomicroscope. Images were taken of areas containing the discs and non-treated regions. Each group contained seven embryos (calculated with PS 3.0.5 software, effect size of 50%, standard deviation of 30%, statistical power of 0.8, and $\alpha=0.05$). The CAM assay was completed two times.

Image Analysis - Images were analyzed with Image-Pro Plus software. Blood vessel length and branching number were utilized to measure the effect of SsnB on angiogenesis. The vessel length was measured for areas containing the discs and non-

treated regions. Normalized vessel length was calculated by dividing the length values of the treated regions by those of the non-treated regions. The same process was repeated for measuring the branching number.

Statistical Analysis - To determine if a statistically significant difference between the treatment groups in each experiment existed, a one-way analysis of variance test (ANOVA) was completed.

Results

SsnB inhibits angiogenesis in the CAM assay - Initial *in vitro* studies with SsnB and endothelial cells have demonstrated the ability of SsnB to inhibit important cellular aspects of angiogenesis, including tube formation, cell migration, cell cycle progression, and chemotaxis. However, these *in vitro* results were not conclusive in proving the anti-angiogenic properties of SsnB. We utilized a chick chorioallantoic membrane assay to successfully demonstrate that SsnB inhibits *ex vivo* angiogenesis. The results from the CAM assay are depicted in Figure 3.2. Overall, SsnB resulted in a significant decrease in normalized blood vessel length compared to the vehicle control group (ANOVA, $p < 0.05$).

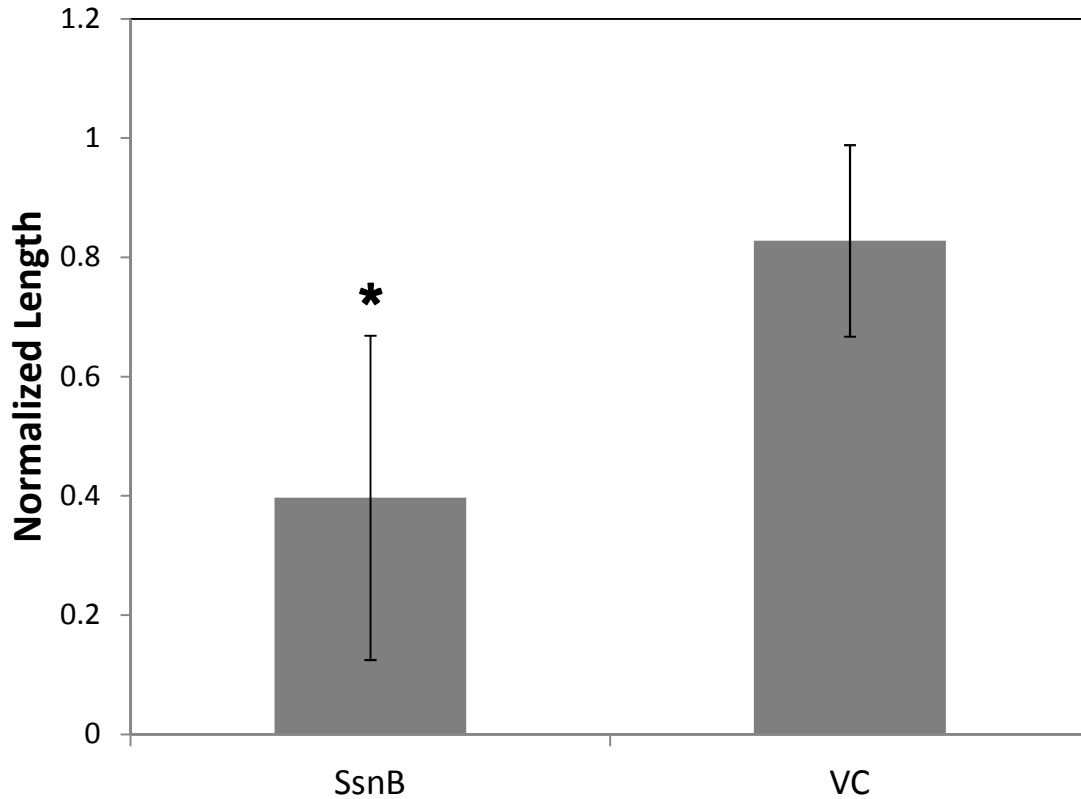


Figure 3.2 SsnB reduces normalized blood vessel length in the CAM assay.

In addition to inhibiting blood vessel length, SsnB also caused a significant decrease in the normalized branch number. The results are depicted in Figure 3.3. Compared to the vehicle control, SsnB decreased the number of points where blood vessels branched into two or more separate vessels. Interestingly, it has been shown that macrophage production of matrix metalloproteinases is important for blood vessel branching. SsnB may be inhibiting this process by blocking TLR activation of macrophages.

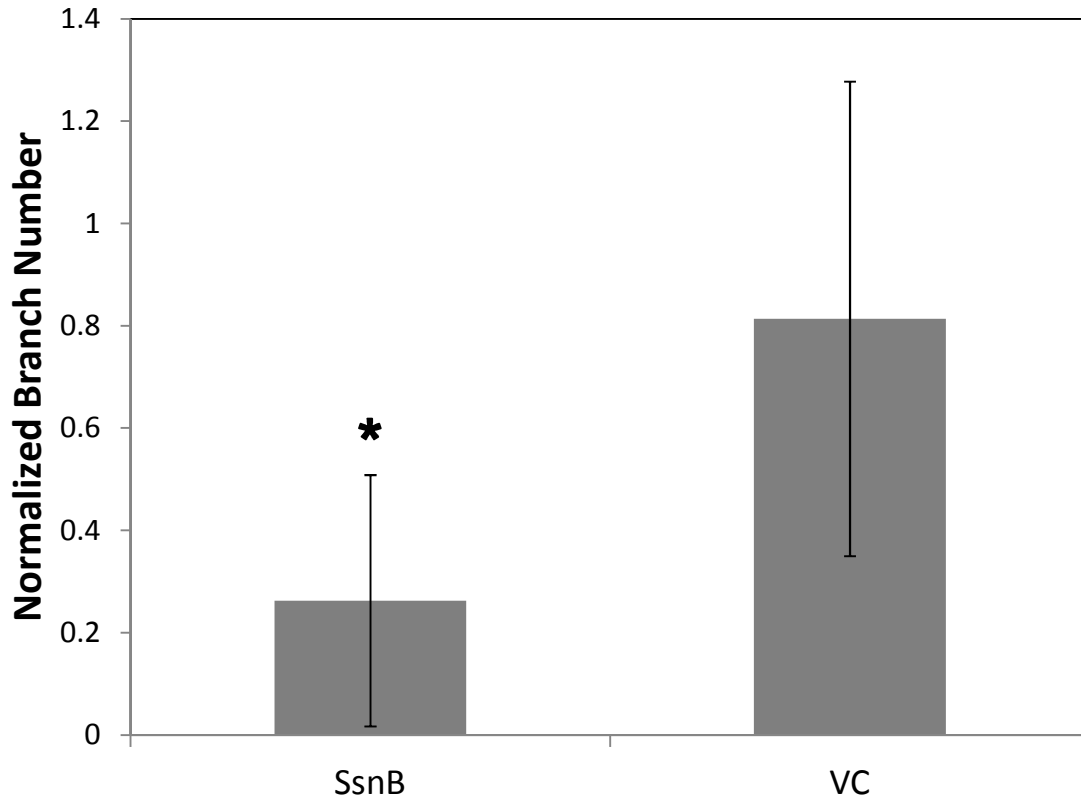


Figure 3.3 SsnB reduces normalized branch number in the CAM assay

Representative images of the CAM from the SsnB and vehicle control groups after two days of treatment are shown in figure 3.4. The methylcellulose discs released SsnB or vehicle control and were still present at the end of the experiment, as complete biodegradation did not occur. The transparency of the methylcellulose discs allowed easy imaging of the vascular network underneath the discs. Images were taken of regions of the CAM that received methylcellulose discs as well as regions that did not receive discs. For each embryo, the blood vessel length and branch number were measured for both treated and non-treated areas. A normalized value was calculated by dividing the treated areas by the non-treated areas. This approach allowed us to compensate for natural variations in vascular density among embryos that normally occur without the presence of angiogenic inhibitors or stimulators. Overall, the SsnB-treated group showed

fewer blood vessels, smaller vessel lengths, and fewer branches. The methylcellulose discs with SsnB not only inhibited angiogenesis in the area underneath the disc, but also demonstrated inhibition in the immediate area surrounding the discs. Compared to the SsnB group, the vehicle control group exhibited higher vessel lengths, more vessels, and more vascular branching. Furthermore, SsnB treatment was associated with a decrease in blood vessel diameter and size.

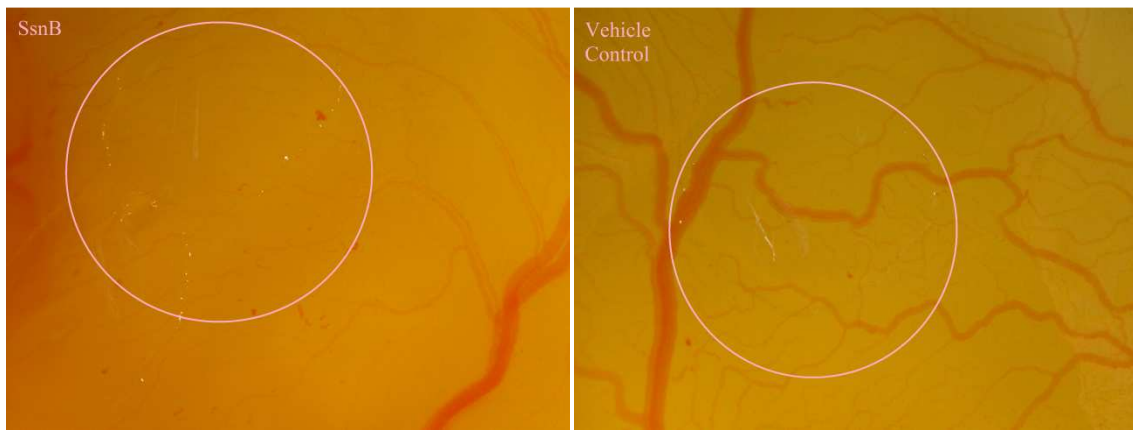


Figure 3.4 Representative images from CAM assay.

In addition, SsnB had no effect on the viability or morphology of the embryos relative to the vehicle control. Both groups experienced similar number of embryo deaths, which is typically encountered with the CAM assay. The embryos that survived until the end of the experiment exhibited no obvious differences in size or morphology between the two groups.

Discussion

We demonstrated that SsnB inhibits endothelial cell functions related to angiogenesis in several *in vitro* functional assays. The data suggests the potential of SsnB as an anti-angiogenic agent by showing inhibition of human endothelial cell tube

formation, migration, and chemotaxis. We have also found evidence supporting the cytostatic nature of SsnB by showing that it inhibits endothelial cell progression through the cell cycle. In this work, we have also demonstrated that SsnB inhibits *ex vivo* angiogenesis in the CAM assay.

Angiogenesis is a complex process comprised of numerous steps. The process is initiated by endothelial activation, often by growth factors, such as VEGF and FGF. Activated endothelial cells proliferate, secrete proteases, and migrate, eventually forming capillary tubes with complete lumens. Each of these steps may serve as a potential target for anti-angiogenic agents. SsnB is capable of inhibiting angiogenesis by targeting multiple steps in the angiogenesis pathway (Roy et al. 2006). We have previously shown that SsnB is capable of inhibiting tube formation and cell migration in the Matrigel tube assay and Transwell insert migration assay, respectively. We have also shown SsnB arrests endothelial cell division in the G1 phase of the cell cycle with associated downregulation of the cell cycle regulatory proteins, cdc6 and cyclin E2. This cell cycle arrest allows SsnB to act as a cytostatic agent, slowing endothelial division. Finally, we have shown that SsnB inhibits *ex vivo* angiogenesis in the CAM assay. The evidence to date suggests that SsnB is an effective inhibitor of angiogenesis, and may prove to be a suitable therapeutic alternative to treat disorders in which excessive blood vessel growth contributes to the pathology, including cancer, rheumatoid arthritis, and psoriasis (Mombeinipour et al. 2013). SsnB may particularly be suited to treat atherosclerosis due to its combined anti-angiogenic and anti-inflammatory properties. Inhibiting angiogenesis may prevent intraplaque angiogenesis, thereby limiting plaque growth, destabilization, and subsequent rupture. At the same time, SsnB may inhibit the chronic

inflammatory reactions necessary for plaque formation and growth (Moreno et al. 2004; Virmani et al. 2005).

SsnB is derived from the plant, *Sparganium stoloniferum*, an aquatic herb that has been used to treat a multitude of disorders including cancer. Past research with this herb has demonstrated its use to treat cancer, seizure disorders, and inflammatory diseases (Wu et al. 2012). Especially relevant to our research, Sun et al demonstrated the anti-angiogenic effects of an aqueous extract from *Sparganium stoloniferum*. In their research, pregnant mice were administered the aqueous extract, and the offspring from these mice were examined and compared to controls. The offspring exhibited numerous morphological abnormalities, related to disrupted angiogenesis and estrogen signaling, including limb, heart, vertebral, and craniofacial defects. FGF and VEGF levels were lowered in the offspring, causing decreased angiogenesis. A disruption in FGF signaling is also known to cause defects in limb bud and cranial formation and heart development. Anti-estrogen activity was implicated in increased numbers of male offspring relative to female offspring. The aqueous extract utilized in Sun's research contained a multitude of active components (Sun, Wang, and Wei 2011). Our research only focused on one particular active compound from *Sparganium stoloniferum*.

Prior research with SsnB has demonstrated its ability to inhibit inflammation. Specifically, SsnB was shown to inhibit Toll-like Receptor 2 (TLR-2) and Toll-like Receptor 4 (TLR-4) mediated inflammation, by acting as an antagonist to both receptors. Inflammatory cytokine production from lipopolysaccharide (LPS)-treated macrophages and mice was inhibited by SsnB treatment. SsnB inhibits toll-like receptors intracellularly, somewhere between ligand binding and immediate adaptor recruitment

(for example, MyD88). SsnB may act directly on TLR2 and TLR4 TIR domains or TIRAP/mal protein, which is an indispensable adaptor bridging TLR2/TLR4 TIR domain and MyD88 interaction (Liang et al. 2011). Toll-like receptors are mainly involved in the innate immune system, where they activate inflammatory pathways to deal with pathogens. However, toll-like receptors have also been shown to be implicated in cancer cell proliferation and metastasis. Functional TLRs are expressed on many different tumor cell types; their activation stimulates cell proliferation and escape from apoptosis. TLRs may also enhance expression and activation of metalloproteinases and integrins, resulting in increased cancer cell invasion and metastasis. TLR signaling may also provide cancer cells with resistance to the host immune system through upregulation of immunosuppressive molecules and inhibitory cytokines (Huang et al. 2008). Overall, SsnB blocks the TLR signaling pathway, preventing many of the steps described above, some of which are also important in angiogenesis. Thus, it is conceivable that SsnB may block cancer progression by multiple mechanisms in addition to inhibiting angiogenesis.

SsnB crosses the cell membrane and works intracellularly to suppress signaling pathways. Previously published data has shown that SsnB can suppress the NF- κ B pathway, and prior studies have demonstrated a link between NF- κ B signaling and expression of cell cycle proteins. Genes for these regulatory proteins, such as CCNE2, CDC6, CCNB1, and CDC2, contain binding sites for NF- κ B. SsnB may suppress the NF- κ B pathway and cause a subsequent downregulation of the cell cycle regulatory proteins CCNE2 and CDC6. SsnB has also been shown to inhibit the MAPK pathways, including JNK, ERK, and p38 signaling, which all affect gene expression and cell proliferation. In the future, we need to explore these relationships as potential

mechanisms of angiogenesis inhibition (Hsu, Lee, and Pan; Cude et al. 2007; Liu et al. 2009; Wang et al.; Meteoglu et al. 2008; Liang et al. 2011).

We hypothesize that the main activity of SsnB involves a cytostatic effect whereby it limits endothelial cell cycle progression by trapping cells in the G1 phase of the cell cycle. This is accomplished by downregulating two key regulatory proteins, cdc6 and cyclin E2, that are necessary to progress beyond the G1/S checkpoint. As a result endothelial cell progression through the cell cycle is slowed down, limiting necessary cell proliferation required for angiogenesis. Emodin, a structurally similar plant-derived polyphenol, has also been shown to inhibit angiogenesis by targeting endothelial cell proliferation (Kwak et al. 2006). Emodin causes a downregulation of CCNB1 and CDC2 and a cell cycle arrest at the G2/M phase (Wang, Wu, and Zhen 2004).

In addition, we also hypothesize that SsnB may inhibit endothelial cell migration and tube formation, additional steps required for angiogenesis, by modulating cytoskeletal reorganization. The microarray data for both HUVECs and HCAECs demonstrates an enrichment of genes associated with cell motility and cytokinesis, including cytoskeleton associated protein 2-like (CKAP2L), diaphanous homolog 3 (DIAPH3), hyaluronan-mediated motility receptor (HMMR), and anillin (ANLN), an actin binding protein. All four genes are involved with the cytoskeleton, cytokinesis, and stress fiber formation (Piekny and Maddox 2010; Yang et al. 2007; Yang et al. 2010). In the tube formation experiments, SsnB seemed to change cell shape, and this may be caused by changes in the cytoskeleton. We need to further investigate how SsnB affects endothelial cell shape, cytoskeleton arrangement, and stress fiber formation, and how cytoskeletal effects interact to reduce cell migration and tube formation.

Furthermore, the CAM assay allowed us to examine the effects of SsnB on additional cell types beyond endothelial cells. Multiple cell types are involved in angiogenesis, including endothelial cells and supporting cells, such as pericytes, smooth muscle cells, macrophages, and myofibroblasts. Since our initial *in vitro* experiments only involved endothelial cells, we utilized the CAM assay to address the multicellular nature of angiogenesis. We are particularly interested in how SsnB affects macrophages. In the CAM assay, SsnB inhibited blood vessel branching. It has been demonstrated that macrophage production of matrix metalloproteinase-9 (MMP-9) plays an important role in vascular branching during neovascularization (Johnson et al. 2004). Prior research has shown that SsnB blocks TLR-2 and TLR-4 mediated inflammation in human and murine macrophages. Furthermore, TLR signaling activates MMP production in macrophages (Huang et al. 2008). We hypothesize that SsnB blocks TLR signaling and subsequently inhibits macrophage MMP-9 production required for blood vessel branching. Additional experiments could examine this relationship between SsnB, TLR signaling, macrophage production of MMP-9, and vascular branching.

Overall, SsnB exhibits many diverse effects, including anti-angiogenic, and cytostatic properties, which may contribute in part to the traditionally reported results of treatment with *Sparganium stoloniferum* and its extracts.

CHAPTER 4

DISCUSSION

Angiogenesis plays an important role in physiological and pathological processes. Unregulated angiogenesis contributes to many pathological conditions, such as rheumatoid arthritis, psoriasis, retinopathy, and tumor growth and metastasis. Angiogenesis also plays a significant role in atherosclerosis. Capillary networks within atherosclerotic plaques can serve as a source of inflammatory cells and mediators, promoting plaque formation. Recent research has suggested that inhibiting angiogenesis may improve plaque stability and decrease plaque formation by limiting this supply of necessary factors to the growing plaque (Griffioen and Molema 2000).

Complementary and alternative medicine is a growing area of research which may hold the key to treatment of numerous disorders, including ones associated with angiogenesis. Researchers have often looked towards herbal medicine, which has been used in many countries throughout the world for centuries, for sources of biologically active molecules. Herbal remedies play a large role in Traditional Chinese Medicine, where plants and plant-derived extracts and compounds are used to treat a multitude of disorders. Many plants secrete bioactive compounds as a defense mechanism to deal with pests. These bioactive compounds exhibit an array of effects, including cytotoxic or cytostatic properties. Many modern day drugs have been isolated and characterized from these plants, which have played a large role in Traditional Chinese Medicine (Qin and Xu 1998; Zhou and Wu 2006).

One such herb, *Sparganium stoloniferum*, has been extensively used in Chinese herbal medicine to treat a variety of disorders, including seizures, amenorrhea, and cancer. *Sparganium stoloniferum* is an aquatic plant which grows in the northern and eastern regions of China (Wu et al. 2012; Sun, Wang, and Wei 2011). Sparstolonin B, a bioactive compound isolated from *S. stoloniferum*, has already been shown to act as a potent anti-inflammatory agent. In experiments with mouse and human macrophages, SsnB inhibited Toll-like receptor (TLR) 2 and 4 mediated inflammation, decreasing cytokine release. SsnB crosses the cell membrane and inhibits the TLRs by blocking MyD88 recruitment, an important step in TLR signaling. SsnB belongs to the polyphenol family of compounds; its structure is similar to isocoumarin and xanthone, both strong anti-inflammatory compounds (Liang et al. 2011).

We have demonstrated the potential of Sparstolonin B as an inhibitor of angiogenesis. SsnB inhibited angiogenesis-related cell activities in functional assays *in vitro*, altered the expression of angiogenesis related genes, and inhibited *ex vivo* angiogenesis. The first part of the project showed that SsnB inhibited angiogenic activities of endothelial cells in functional assays, including the Matrigel tube formation assay and the Transwell cell migration assay. In the second part of the project, we utilized microarrays and qRT-PCR to demonstrate that SsnB altered the expression of genes in HUVECs and HCAECs related to cell cycle progression, cytokinesis, nuclear division, cytoskeleton, and chemotaxis, all important pathways in angiogenesis. We were especially interested in the downregulation of the cell cycle proteins CCNE2 and CDC6, which control progression through the G1/S checkpoint. Using flow cytometry, we demonstrated that SsnB blocked cell cycle progression at this checkpoint. In the third

part of the project, we showed that SsnB blocked *ex vivo* angiogenesis in the chick chorioallantoic membrane assay. Overall, SsnB may prove to be a successful alternative therapy for angiogenesis-related disorders, including cancer, rheumatoid arthritis, and atherosclerosis.

SsnB inhibits angiogenic functions in endothelial cells

In the first part of the project, we demonstrated that SsnB inhibits endothelial cell activity in several functional assays. SsnB caused a dose-dependent reduction of total tube length in the Matrigel tube formation assay with HUVECs, HCAECs, and HMVECs. Increasing the concentration of SsnB from 1 to 100 micromolar increased the level of inhibition compared to the vehicle control. In all the SsnB treatment groups, the endothelial cells showed morphological changes, including cell rounding and clumping. We initially believed that this might be a sign of cell death or apoptosis induced by SsnB. However, a live/dead assay showed that SsnB had no effect on cell viability. In all SsnB treatment groups, we observed no cell death; all cells stained positively for viable cells. We hypothesize that SsnB is affecting pathways related to cell morphology and motility. Anti-angiogenic agents often inhibit cell motility by targeting the actin cytoskeleton and microtubule system (Karna et al. 2012). SsnB may be acting in this manner, preventing the necessary changes in cell shape and movement necessary for tube formation in the Matrigel assay. This would also explain the changes in morphology and cell clumping seen in our Matrigel assays.

In addition, SsnB treatment resulted in a dose-dependent inhibition of endothelial cell migration in the Transwell insert assay. HUVECs and HCAECs experienced a dose-

dependent inhibition in migration in response to SsnB concentrations from 0.0001 and 0.1 μM that reached a plateau between 0.1 and 100 μM of SsnB. The cell migration assay relied upon VEGF-directed chemotaxis. Therefore, SsnB must somehow interfere with chemotaxis, through mechanisms which could range from inhibition of VEGF signaling to impaired cell motility or adhesion. Our microarray datasets demonstrated an enrichment in genes associated with chemotaxis, cytoskeleton, and cell adhesion, which may provide clues as to how SsnB inhibits cell migration. Perhaps SsnB is causing endothelial cells to adopt an adhesive state, limiting chemotaxis. Compared to the Matrigel tube formation assay, the cell migration assay demonstrated a dose-dependent inhibition at lower concentrations of SsnB (between 0.0001 and 0.1 μM), which reached a plateau at 0.1 μM . This may indicate that cell migration is more sensitive to SsnB exposure compared to tube formation.

The inhibition in tube formation and cell migration by SsnB may involve targeting the cell motility apparatus through alterations in the actin cytoskeleton and microtubule system. The cytoskeleton is the main driving force for cell movement and shape change. Actin is the key component of the cytoskeleton, which controls cell locomotion. Cellular movement involves a coordinated effort of actin polymerization and depolymerization, as well as focal adhesion assembly and disassembly.

Microtubules interact with the actin cytoskeleton, provide structural support, and play a key role in establishing cell polarity and centrosome orientation. These processes help establish a leading edge in the cell that is utilized for directed movement. Intermediate filaments, including vimentin, are important components of the cytoskeleton, providing cell shape and participating in interactions between actin filaments and microtubules.

Stress fibers and focal adhesions are additional structures associated with the cytoskeleton that play a strong role in cell movement and migration. Stress fibers represent organized centers of actin filaments, myosin, and intermediate filaments that generate force for cell movement, migration, and adhesion. Focal adhesions are complex protein structures through which the cytoskeleton interacts with the extracellular matrix, establishing attachment points with the ECM as cell movement occurs. Cell movement is comprised of three distinct phases (protrusion, attachment, and traction) that all incorporate interactions between microfilaments, microtubules, stress fibers, and focal adhesions. Cell motility begins with the protrusion of lamellopodia from the leading edge of the cell, mainly through actin polymerization. As the lamellopodia extend across the underlying surface, the cell attaches and detaches to ECM components through specialized receptors, including integrins. During traction, the bulk of the cell is carried forward toward the leading edge. Overall, any disruptions in the cytoskeleton or associated structures lead to inhibition of cell mobility (Fenteany and Zhu 2003; Lamalice, Le Boeuf, and Huot 2007; Mackay 2008).

Some naturally derived compounds target the actin cytoskeleton or microtubules to inhibit cytoskeleton dependent functions, including cell migration. They may inhibit actin / microtubule polymerization leading to cytoskeleton destabilization, or promote actin / microtubule polymerization leading to cytoskeleton stabilization. In both cases, cell motility becomes limited due to disruption in normal cytoskeleton functioning, ultimately inhibiting processes, such as angiogenesis, that depend on cell movement. Cytochalasins, a group of fungally derived molecules, bind the barbed ends of microfilaments and block polymerization and depolymerization, effectively capping the

growing end and preventing extension of actin filaments into the leading edge of the cell. Phalloidin, another fungally derived compound, stabilizes actin filaments, promotes actin polymerization, and inhibits depolymerization, locking actin filaments in place (Fenteany and Zhu 2003). Compounds that target microtubules include taxanes and epothilones, which inhibit tubulin depolymerization and promote microtubule stabilization, and vinca alkaloids that inhibit polymerization and mitotic spindle formation (Bijman et al. 2006). In addition, compounds may also target upstream signaling pathways that control microfilaments and microtubules. Intracellular targets for microfilament and microtubule disruption include Rho GTPases, a family of signaling molecules that control cell motility. Tumor-derived VEGF has been shown to activate Rho GTPases, including Cdc42, Rac1, and RhoA. Once activated, these signaling molecules affect cytoskeletal organization, including filopodia, lamellipodia, and stress fibers, all impacting cell shape and motility. Furthermore, cdc42 affects the orientation of the centrosome and cell polarity, RhoA controls actin-myosin contraction promoting cell movement, and Rac1 promotes actin polymerization in the leading edge and focal adhesion formation. Inhibition of these signaling molecules leads to disruptions in the cytoskeleton, stress fiber formation, and focal adhesion. Many of these inhibitory compounds possess polycyclic structures and functional groups similar to SsnB (Vincent et al. 2001; Fenteany and Zhu 2003; Karna et al. 2012). Based on the results from the cell migration and tube formation experiments, as well as the microarray data described below, we believe that SsnB may act in part by targeting the cytoskeleton or upstream signaling pathways to impede changes in cell shape and motility that are both necessary for angiogenesis.

SsnB alters endothelial gene expression and limits cell cycle progression

We also demonstrated that SsnB altered the expression of genes implicated in angiogenesis. Microarray data from human umbilical vein endothelial cells and human coronary artery endothelial cells showed altered expression in genes associated with a variety of biological processes, including cell division, cell cycle progression, chemotaxis, and cytoskeleton, which may provide insight into the results seen in the tube formation and cell migration experiments. The majority of the enriched genes are also associated with mitosis. Many genes that are usually upregulated during progression through the cell cycle to mitosis were downregulated in our microarray data, including genes such as anillin (ANLN), cyclin E2 (CCNE2), cell division cycle 6 (CDC6), cyclin B1 (CCNB1), cyclin dependent kinase 1 (CDC2), and aurora kinases A and B (AURKA, AURKB) (Dephoure et al. 2008). Clearly, SsnB has shown a strong effect on mitosis and the events preceding mitosis. Downregulation of these genes may hinder the necessary cell division and proliferation that is required for angiogenesis. Based on our cell cycle experiments, we believe that SsnB is causing blockage at two checkpoints in the cell cycle, the G1/S and G2/M checkpoints, with the former checkpoint dominating. Overall, the microarray data supported the results of our functional assays and provided insight into the mechanism of inhibitory action through pathways including cell cycle progression, cytoskeleton alterations, and chemotaxis.

The genes from the microarray data that initially captured our attention were those involved in the cell cycle. Table 2.1 demonstrates that CCNE2, CDC6, CCNB1, and CDC2 were all downregulated by SsnB. Cyclins are regulatory proteins that bind and activate cell dependent kinases, most importantly cyclin dependent kinase 2 (CDK2),

which phosphorylate additional proteins, initiating a cascade of cellular events that prepare the cell for mitosis and division. Cyclin levels rise and fall depending on the phase of the cell cycle. Normally, CCNE2 and CCNB1 rise in the G1/S and G2/M phases, respectively. CCNE2 binds and activates CDK2, which phosphorylates retinoblastoma protein, allowing it to dissociate from the E2F transcription factor. E2F is then free to activate gene transcription and promote progression through the G1/S checkpoint. CDC6 plays an essential role in chromosome duplication during the S phase. CCNB1 binds and activates CDC2 during progression through the G2/M checkpoint, preparing the cell for mitosis (Wu et al. 2009; Borlado and Mendez 2008). The downregulation of CCNE2 and CDC6 directly supports the G1/S blockage observed in our cell cycle experiments with synchronized endothelial cells. We believe that SsnB is downregulating CCNE2 and CDC6, slowing progression through the G1/S checkpoint. The microarray data also showed a downregulation of CCNB1 and CDC2, which should trap cells at the G2/M checkpoint and prevent endothelial cells from entering the final stages of cell division. This effect was less readily seen due to blockage at the G1/S checkpoint. In non-synchronized (no serum starvation) HUVECs, G2/M blockage was observed (see Appendix, Figure A.5) but at much lower levels compared to the G1/S blockage.

In addition to the cell cycle regulatory genes, there were additional genes associated with mitosis and the cytoskeleton that stood out in our microarray data. The microarray data showed an enrichment in genes encoding proteins associated with the spindle, nuclear envelope, chromosome condensation and segregation, and cytokinesis, all important aspects of mitosis and cell division. SsnB caused a downregulation in the

expression of anillin (ANLN), an actin binding protein that plays an important role in cytokinesis, the final stage of cell division. This could inhibit contractile ring formation, preventing the cytoskeletal changes necessary for cytokinesis (Piekny and Maddox 2010). Decreased expression of anillin might explain the nuclei clumping or double nuclei that we observed in additional experiments (see Appendix Figure A.6) with nuclear staining (Hoechst). Our microarray data also contained many examples of differentially downregulated cytoskeleton- related genes, including transforming acidic coiled-coil containing protein 3 (TACC3), hyaluronan-mediated motility receptor (HMMR), and diaphanous homolog 3 (DIAPH3). Downregulation of the protein products of these genes may have a negative influence on cytoskeleton functioning, which is essential for not only mitosis and cytokinesis, but for cell motility as well. DIAPH3 is an essential element in filopodia and lamellopodia formation, both important processes for cell motility. Downregulation of DIAPH3 may inhibit lamellopodia / filopodia protrusion and subsequent cell spreading (Yang et al. 2007). This may explain the cell rounding that we noticed in the tube formation experiments. TACC3 mainly controls microtubules and is intricately involved with the centrosome and mitotic spindle apparatus during mitosis. The spindle apparatus is required for separation of sister chromatids and subsequent nuclear division. Any disruption of this process could negatively affect cell proliferation. Furthermore, aurora kinases (AURKA and AURKB), which were also downregulated in our data, help regulate TACC3-mediated formation of the mitotic spindle apparatus (Piekorz et al. 2002; Kinoshita et al. 2005). Hyaluronan-mediated motility receptor (HMMR or RHAMM) is a protein that regulates microtubule function during mitosis and the turnover of focal adhesions. RHAMM has been shown to

be important for endothelial cell migration during angiogenesis. Antibodies directed against RHAMM effectively inhibited angiogenesis associated with cancer (Yang et al. 2010). RHAMM was also downregulated in our microarray data, suggesting its involvement in the inhibition of endothelial cell migration and angiogenesis seen in our experiments.

Kinesin family member 18A (KIF18A) is another gene that was downregulated in our microarray data. Its functions encompass a variety of pathways, including the cytoskeleton, cell cycle progression, and cell division, which are all the main mechanistic processes that we believe SsnB targets to inhibit angiogenesis. KIF18A is a molecular motor that produces force and movement along microtubules to aid in cytoskeleton rearrangement, especially chromosome movement. KIF18A has also been shown to interact with caveolin-1 (CAV1) (Luboshits and Benayahu 2005, 2007). Caveolin-1 is involved in cellular pathways associated with cell morphology and stress fiber formation. Silencing of caveolin-1 has been shown to inhibit angiogenesis through multiple mechanisms including alterations in cell morphology (increased cell size and stress fiber formation) and inhibition in cell migration and progression through the G1/S checkpoint. These findings connect especially well with our results since we demonstrated a similar behavior in endothelial cells in response to SsnB treatment. We hypothesize that SsnB may inhibit caveolin-1-mediated activities through downregulation of KIF18A. Caveolin-1 also signals through the AKT pathway; SsnB may somehow interfere with this signaling pathway (Madaro et al. 2013). Prior research has shown that SsnB inhibits NF- κ B, ERK, JNK, and p38 pathways in macrophages. Inhibition of the AKT pathway may be another mechanism to inhibit caveolin-1-mediated signaling. Further research is

necessary to test this hypothesis. Overall, the combined effects of inhibiting cell cycle progression, cytokinesis, mitosis, and cytoskeletal function help explain the cytostatic and anti-angiogenic properties of SsnB.

SsnB inhibits ex vivo angiogenesis

In the final portion of the research project, we utilized the chick chorioallantoic membrane assay to examine the effects of SsnB on *ex vivo* angiogenesis. Methylcellulose discs containing either 100 μ M SsnB or vehicle control (0.1% DMSO) were added to the CAM of chicken eggs. After incubation for two days, the blood vessel length and branching pattern were examined. SsnB caused a significant reduction in total blood vessel length compared to the vehicle control group, successfully demonstrating the ability of SsnB to inhibit *ex vivo* angiogenesis. We also demonstrated that SsnB reduced the number of branch points in developing blood vessels.

The CAM assay incorporates multiple cell types, unlike *in vitro* functional assays. *In vitro* assays, including the Matrigel tube formation assay, only examine the effects of a test compound on one isolated cell type, namely endothelial cells. Oftentimes, a compound that exhibits anti-angiogenic properties with *in vitro* functional assays may not inhibit *in vivo* or *ex vivo* angiogenesis. Furthermore, compounds such as SsnB may inhibit angiogenesis by targeting additional cell types, and this type of interaction can be revealed by *in vivo* / *ex vivo* assays. Angiogenesis is a multicellular process involving multiple cell types including endothelial cells and supporting cells, such as pericytes, smooth muscle cells, myofibroblasts, and macrophages. For example, pericytes and myofibroblasts help produce collagen fibers to create a framework for vessel formation

during splitting or intussusceptive angiogenesis, and macrophages produce matrix metalloproteinases that degrade the basement membrane, providing a path for cell migration. Normal angiogenesis also involves cell interactions with the extracellular matrix, which are not properly addressed by *in vitro* assays. Moreover, cultured endothelial cells have been preselected by passaging to adopt a proliferative phenotype, which is uncharacteristic of *in vivo* angiogenesis. The CAM assay includes multiple cell types and extracellular matrix interactions to address all of these issues associated with *in vitro* assays (Ribatti 2008; Cimpean, Ribatti, and Raica 2008). Using the CAM assay, we demonstrated that SsnB effectively inhibited angiogenesis, by decreasing total blood vessel length and by reducing branch number. This data demonstrates that SsnB is capable of inhibiting true, physiological angiogenesis.

Interestingly, SsnB caused a significant reduction in the number of branches in the developing CAM blood vessels. Blood vessel branch points have been shown to colocalize with macrophages that secrete matrix metalloproteinases (MMP) which are necessary for establishing these branch points. MMPs, especially MMP-9, help degrade the extracellular matrix, providing access routes for endothelial cells to migrate through the ECM to create new branches from the original blood vessels as angiogenesis progresses (Johnson et al. 2004). The observed decrease in CAM vessel branching may reflect an inhibitory action on macrophages by SsnB. Previous research has shown that SsnB is capable of inhibiting macrophage-mediated inflammation by blocking toll-like receptor signaling. In addition to its effects on endothelial cells, SsnB may also be inhibiting macrophage production of MMPs or other proteolytic enzymes, thereby reducing the density of branching usually seen in angiogenesis in the CAM assay.

Limitations and Future Work

Although our research has yielded promising results in demonstrating the anti-angiogenic potential of SsnB, our results are still constrained by limitations associated with our experimental models. Initial experiments with SsnB only utilized *in vitro* assays to investigate endothelial cells, leaving out supporting cells involved in angiogenesis, including macrophages, pericytes, and smooth muscle cells. Our *in vitro* assays also only investigated three functional aspects of angiogenesis: chemotaxis, tube formation, and cell cycle progression. Since our microarray data contained such a large number of differentially regulated genes associated with the cytoskeleton, it would be beneficial to investigate how SsnB alters the cytoskeleton and how this impacts chemoattractant driven angiogenesis. We could begin by studying how SsnB alters stress fiber formation and cell shape through phalloidin staining. This would be helpful in examining the cell shape changes that were seen in the tube formation experiment. We may also study how SsnB affects focal adhesion formation with staining for integrins or associated proteins, such as vinculin (Wickstrom, Alitalo, and Keski-Oja 2004). This would begin to address the question of whether SsnB is impeding cell migration by causing the endothelial cells to adopt an adhesive phenotype. Both of the preceding experiments may be utilized concurrently with a scratch wound healing assay to further investigate the effects on chemotaxis. In addition, assays with multiple cell types, including supporting smooth muscle cells or pericytes, may be utilized to examine the impact of SsnB on additional cell types (Suboj et al. 2012). We may also examine how SsnB affects macrophages in relation to angiogenesis, including metalloproteinase production. This would expand upon the results that we saw in the CAM assay in regards to branching inhibition.

We utilized the CAM assay as an *ex vivo* assay to investigate the effects of SsnB in a multicellular environment, incorporating interactions with the ECM. However, the CAM assay also has associated limitations. The CAM assay is not a mammalian assay; differences exist between chicken cells and mammalian cells. Since chick embryos do not have a mature immune system until the late stages of incubation, specific interactions between SsnB and lymphoid cells, such as T and B lymphocytes, cannot be examined. Furthermore, nonspecific inflammatory reactions to the methylcellulose discs may occur as activated macrophages release inflammatory cytokines in response to added compounds. In addition, the CAM is undergoing constant morphological changes, including contraction, that may alter the vascular density independent of the tested compound (Ribatti 2008). The *ex ovo* version of the CAM assay employed in this project also exhibited a high mortality rate in embryo survival. The Matrigel plug assay may be used to overcome these problems and to provide additional support for our findings from the CAM assay. The Matrigel plug assay is widely used to study *in vivo* angiogenesis. The assay is simple, reproducible, and reveals more important information than *in vitro* assays, such as the Matrigel tube formation assay. In this assay, Matrigel is injected subcutaneously in mice. Over time, endothelial cells from each host mouse invade the Matrigel plugs, producing capillary networks. Drug delivery pumps may be subcutaneously implanted in the mice during this period to study how test compounds affect angiogenesis. After enough time has progressed for capillary formation to occur within the Matrigel, the mice are injected intravenously with Dextran-FITC to allow visualization and quantification of vessel formation. After removing the plugs, the gross vessel distribution is noted with a fluorescent dissecting scope, and fluorescent images

are collected and analyzed (Staton, Reed, and Brown 2009). SsnB is expected to decrease the number of capillaries that grow into the Matrigel plugs as it has shown the ability to inhibit angiogenesis for *in vitro* models and the CAM model. Furthermore, this assay could provide additional insight into the effects of SsnB on capillary structure and cell composition. This will provide a more complete picture of how SsnB affects multiple mammalian cell types, including immune cells.

The Matrigel plug assay only stimulates the growth of capillaries. The hindlimb ischemia model may be used as an *in vivo* assay for angiogenesis and arteriogenesis. In this model, the femoral artery in the hindlimb of the mouse is ligated to provide an area of ischemia that will stimulate blood vessel formation and remodeling. Decreased bloodflow in the hindlimb is monitored with Doppler ultrasound. This model stimulates growth of both capillaries and larger caliber vessels, compared to the Matrigel plug assay which only stimulates angiogenesis (van Royen et al. 2001). In our CAM assay, we only studied the effects of 100 μ M SsnB on angiogenesis due to the limited number of embryos that remained viable over the course of the experiment. It would be more ideal to study the effects of several concentrations of SsnB for a dose-response study. This may be accomplished with the Matrigel or hindlimb ischemia assays. For the CAM assay, we based our concentration (100 μ M) on results from the *in vitro* experiments. We may need to carry out a series of preliminary experiments to test the feasibility of different delivery methods (osmotic mini pumps or intraperitoneal injections) for SsnB. These experiments may provide us with more insight into the effective dose ranges of SsnB for different *in vivo* models.

Before beginning additional *in vivo* experiments, it would be especially helpful to determine the pharmacokinetics of SsnB. We need to know more about how SsnB is absorbed through various routes of administration, and which route works best. Using a murine model, we should investigate how SsnB becomes distributed within the body over time. This would show us in which tissues SsnB becomes enriched, providing clues into the bioavailability of SsnB. Furthermore, it would also be interesting to investigate how the body eliminates SsnB through metabolism and excretion. This could demonstrate potential toxic byproducts from metabolic degradation of SsnB. To begin the pharmacokinetic studies, we need to have a method to detect SsnB in plasma and urine samples. SsnB could be conjugated with markers for detection in these assays, or antibodies directed against structural motifs of SsnB could be created for ELISAs or western blots. Overall, SsnB has proven effective in inhibiting angiogenesis in our experiments, but its efficacy could be improved. SsnB may serve as a starting point for derivatized compounds. Functional groups may be added or modified to improve the solubility, bioavailability, and activity of SsnB. These derivatized compounds may also possess additional therapeutic properties (Liang et al. 1995).

In addition, we could learn more about the mechanism of action for SsnB by investigating potential binding sites. An understanding of the initial steps of SsnB binding to endothelial cells will reveal additional details about downstream pathways, confirming our prior microarray data. The Aryl Hydrocarbon Receptor (AHR) seems a likely candidate due to the polycyclic structure of SsnB and the connection between the AHR pathway and inhibition of HIF-1 α -driven angiogenesis. The upregulation of AHR-associated genes, NQO1, ALDH3A1, CYP1A1, and CYP1B1, in our preliminary

microarray data also provides supporting evidence for the Aryl Hydrocarbon Receptor as a binding site for SsnB. The aryl hydrocarbon receptor binds polycyclic and halogenated aromatic hydrocarbons. After AHR binding, the AHR ligand complex and the AHR nuclear translocator (ARNT), also known as hypoxia-inducible factor-1 β (HIF-1 β), form a heterodimeric transcription factor. This complex binds to xenobiotic response elements in the promoter region of target genes. Hypoxia-inducible factor-1 α (HIF-1 α) is another basic helix-loop-helix transcription factor that dimerizes with ARNT and mediates VEGF gene activation during hypoxic conditions. Recent research has suggested a link between AHR-ARNT signaling and the regulation of angiogenesis. The AHR and HIF-1 α both compete for the ARNT; therefore, increased activation of AHR can decrease hypoxia-driven angiogenesis. SsnB possesses a polycyclic structure, making it a potential ligand for the AHR, which may operate through AHR-ARNT signaling to inhibit angiogenesis (Dong, Ma, and Whitlock 1996; Forsythe et al. 1996; Ichihara et al. 2007; Reyes, Reisz-Porszasz, and Hankinson 1992; Schmidt and Bradfield 1996; Wiesener et al. 1998).

Conclusion

In conclusion, Sparstolonin B has shown promise as an effective inhibitor of angiogenesis. We demonstrated that SsnB inhibited angiogenic functions in several functional assays, including tube formation and cell migration. Microarray analysis showed that SsnB caused differential regulation of genes associated with the cell cycle, cell division, and cytoskeleton. We also showed that SsnB hampered progression through the cell cycle at the G1/S checkpoint, possibly by downregulation of CCNE2 and CDC6. SsnB successfully inhibited angiogenesis in the CAM assay, decreasing vessel length and branching. Future work with SsnB will reveal more about its mechanism of

action, including cytoskeletal changes and possible binding sites. Overall, SsnB has proven to be a powerful bioactive compound with a multitude of useful therapeutic effects, including anti-angiogenesis and anti-inflammation.

REFERENCES

- Auerbach, R., R. Lewis, B. Shinnars, L. Kubai, and N. Akhtar. 2003. Angiogenesis assays: a critical overview. *Clin Chem* 49 (1):32-40.
- Bijman, M. N., G. P. van Nieuw Amerongen, N. Laurens, V. W. van Hinsbergh, and E. Boven. 2006. Microtubule-targeting agents inhibit angiogenesis at subtoxic concentrations, a process associated with inhibition of Rac1 and Cdc42 activity and changes in the endothelial cytoskeleton. *Mol Cancer Ther* 5 (9):2348-57.
- Blacher, S., L. Devy, M. F. Burbridge, G. Roland, G. Tucker, A. Noel, and J. M. Foidart. 2001. Improved quantification of angiogenesis in the rat aortic ring assay. *Angiogenesis* 4 (2):133-42.
- Borlado, L. R., and J. Mendez. 2008. CDC6: from DNA replication to cell cycle checkpoints and oncogenesis. *Carcinogenesis* 29 (2):237-43.
- Bussolino, F., A. Mantovani, and G. Persico. 1997. Molecular mechanisms of blood vessel formation. *Trends Biochem Sci* 22 (7):251-6.
- Carmeliet, P. 2003. Angiogenesis in health and disease. *Nat. Med.* 9 (6):653-60.
- Cimpean, A. M., D. Ribatti, and M. Raica. 2008. The chick embryo chorioallantoic membrane as a model to study tumor metastasis. *Angiogenesis* 11 (4):311-9.
- Cude, K., Y. Wang, H. J. Choi, S. L. Hsuan, H. Zhang, C. Y. Wang, and Z. Xia. 2007. Regulation of the G2-M cell cycle progression by the ERK5-NFkappaB signaling pathway. *J. Cell Biol.* 177 (2):253-64.
- Dephoure, N., C. Zhou, J. Villen, S. A. Beausoleil, C. E. Bakalarski, S. J. Elledge, and S. P. Gygi. 2008. A quantitative atlas of mitotic phosphorylation. *Proc Natl Acad Sci U S A* 105 (31):10762-7.
- Dohle, D. S., S. D. Pasa, S. Gustmann, M. Laub, J. H. Wissler, H. P. Jennissen, and N. Dunker. 2009. Chick ex ovo culture and ex ovo CAM assay: how it really works. *J Vis Exp* (33).
- Dong, L., Q. Ma, and J. P. Whitlock, Jr. 1996. DNA binding by the heterodimeric Ah receptor. Relationship to dioxin-induced CYP1A1 transcription in vivo. *J Biol Chem* 271 (14):7942-8.

- Fenteany, G., and S. Zhu. 2003. Small-molecule inhibitors of actin dynamics and cell motility. *Curr Top Med Chem* 3 (6):593-616.
- Folkman, J. 1971. Tumor angiogenesis: therapeutic implications. *N. Engl. J. Med.* 285 (21):1182-6.
- Forsythe, J. A., B. H. Jiang, N. V. Iyer, F. Agani, S. W. Leung, R. D. Koos, and G. L. Semenza. 1996. Activation of vascular endothelial growth factor gene transcription by hypoxia-inducible factor 1. *Mol Cell Biol* 16 (9):4604-13.
- Griffioen, A. W., and G. Molema. 2000. Angiogenesis: potentials for pharmacologic intervention in the treatment of cancer, cardiovascular diseases, and chronic inflammation. *Pharmacol Rev* 52 (2):237-68.
- Hsu, W. H., B. H. Lee, and T. M. Pan. Red mold dioscorea-induced G2/M arrest and apoptosis in human oral cancer cells. *J Sci Food Agric* 90 (15):2709-15.
- Huang, B., J. Zhao, J. C. Unkeless, Z. H. Feng, and H. Xiong. 2008. TLR signaling by tumor and immune cells: a double-edged sword. *Oncogene* 27 (2):218-24.
- Ichihara, S., Y. Yamada, G. Ichihara, T. Nakajima, P. Li, T. Kondo, F. J. Gonzalez, and T. Murohara. 2007. A role for the aryl hydrocarbon receptor in regulation of ischemia-induced angiogenesis. *Arterioscler Thromb Vasc Biol* 27 (6):1297-304.
- Johnson, C., H. J. Sung, S. M. Lessner, M. E. Fini, and Z. S. Galis. 2004. Matrix metalloproteinase-9 is required for adequate angiogenic revascularization of ischemic tissues: potential role in capillary branching. *Circ Res* 94 (2):262-8.
- Karna, P., P. C. Rida, R. C. Turaga, J. Gao, M. Gupta, A. Fritz, E. Werner, C. Yates, J. Zhou, and R. Aneja. 2012. A novel microtubule-modulating agent EM011 inhibits angiogenesis by repressing the HIF-1 α axis and disrupting cell polarity and migration. *Carcinogenesis* 33 (9):1769-81.
- Khurana, R., M. Simons, J. F. Martin, and I. C. Zachary. 2005. Role of angiogenesis in cardiovascular disease: a critical appraisal. *Circulation* 112 (12):1813-24.
- Kinoshita, K., T. L. Noetzel, L. Pelletier, K. Mechtler, D. N. Drechsel, A. Schwager, M. Lee, J. W. Raff, and A. A. Hyman. 2005. Aurora A phosphorylation of TACC3/maskin is required for centrosome-dependent microtubule assembly in mitosis. *J Cell Biol* 170 (7):1047-55.
- Kwak, H. J., M. J. Park, C. M. Park, S. I. Moon, D. H. Yoo, H. C. Lee, S. H. Lee, M. S. Kim, H. W. Lee, W. S. Shin, I. C. Park, C. H. Rhee, and S. I. Hong. 2006. Emodin inhibits vascular endothelial growth factor-A-induced angiogenesis by blocking receptor-2 (KDR/Flk-1) phosphorylation. *Int. J. Cancer* 118 (11):2711-20.

- Lamallice, L., F. Le Boeuf, and J. Huot. 2007. Endothelial cell migration during angiogenesis. *Circ Res* 100 (6):782-94.
- Lee, S. Y., S. U. Choi, J. H. Lee, D. U. Lee, and K. R. Lee. A new phenylpropane glycoside from the rhizome of *Sparganium stoloniferum*. *Arch. Pharm. Res.* 33 (4):515-21.
- Li, S. X., F. Wang, X. H. Deng, and S. W. Liang. A new alkaloid from the stem of *Sparganium stoloniferum* Buch.-Ham. *J. Asian Nat. Prod. Res.* 12 (4):331-3.
- Liang, J. W., S. L. Hsiu, P. P. Wu, and P. D. Chao. 1995. Emodin pharmacokinetics in rabbits. *Planta Med* 61 (5):406-8.
- Liang, Q., Q. Wu, J. Jiang, J. Duan, C. Wang, M. D. Smith, H. Lu, Q. Wang, P. Nagarkatti, and D. Fan. 2011. Characterization of sparstolonin B, a Chinese herb-derived compound, as a selective Toll-like receptor antagonist with potent anti-inflammatory properties. *J Biol Chem* 286 (30):26470-9.
- Liekens, S., E. De Clercq, and J. Neyts. 2001. Angiogenesis: regulators and clinical applications. *Biochem Pharmacol* 61 (3):253-70.
- Liu, F., X. Li, C. Wang, X. Cai, Z. Du, H. Xu, and F. Li. 2009. Downregulation of p21-activated kinase-1 inhibits the growth of gastric cancer cells involving cyclin B1. *Int. J. Cancer* 125 (11):2511-9.
- Luboshits, G., and D. Benayahu. 2005. MS-KIF18A, new kinesin; structure and cellular expression. *Gene* 351:19-28.
- Luboshits, G., and D. Benayahu. 2007. MS-KIF18A, a kinesin, is associated with estrogen receptor. *J Cell Biochem* 100 (3):693-702.
- Mackay, C. R. 2008. Moving targets: cell migration inhibitors as new anti-inflammatory therapies. *Nat Immunol* 9 (9):988-98.
- Madaro, L., F. Antonangeli, A. Favia, B. Esposito, F. Biamonte, M. Bouche, E. Ziparo, G. Sica, A. Filippini, and A. D'Alessio. 2013. Knock down of caveolin-1 affects morphological and functional hallmarks of human endothelial cells. *J Cell Biochem.*
- Meng, H., G. Xing, B. Sun, F. Zhao, H. Lei, W. Li, Y. Song, Z. Chen, H. Yuan, X. Wang, J. Long, C. Chen, X. Liang, N. Zhang, Z. Chai, and Y. Zhao. Potent angiogenesis inhibition by the particulate form of fullerene derivatives. *ACS Nano.* 4 (5):2773-83.

- Meteoglu, I., I. H. Erdogdu, N. Meydan, M. Erkus, and S. Barutca. 2008. NF-KappaB expression correlates with apoptosis and angiogenesis in clear cell renal cell carcinoma tissues. *J. Exp. Clin. Cancer Res.* 27:53.
- Mombeinipour, M., A. Zare Mirakabadi, K. Mansuri, and M. Lotfi. 2013. In vivo and in vitro anti-angiogenesis effect of venom-derived peptides (ICD-85). *Arch Iran Med* 16 (2):109-13.
- Moreno, P. R., K. R. Purushothaman, V. Fuster, D. Echeverri, H. Trusczyńska, S. K. Sharma, J. J. Badimon, and W. N. O'Connor. 2004. Plaque neovascularization is increased in ruptured atherosclerotic lesions of human aorta: implications for plaque vulnerability. *Circulation* 110 (14):2032-8.
- Nam, D., C. W. Ni, A. Rezvan, J. Suo, K. Budzyn, A. Llanos, D. Harrison, D. Giddens, and H. Jo. 2009. Partial carotid ligation is a model of acutely induced disturbed flow, leading to rapid endothelial dysfunction and atherosclerosis. *Am J Physiol Heart Circ Physiol* 297 (4):H1535-43.
- Nigg, E. A. 2001. Mitotic kinases as regulators of cell division and its checkpoints. *Nat. Rev. Mol. Cell Biol.* 2 (1):21-32.
- O'Farrell, P. H. 2001. Triggering the all-or-nothing switch into mitosis. *Trends Cell Biol.* 11 (12):512-9.
- Pandya, N. M., N. S. Dhalla, and D. D. Santani. 2006. Angiogenesis--a new target for future therapy. *Vascul Pharmacol* 44 (5):265-74.
- Piekny, A. J., and A. S. Maddox. 2010. The myriad roles of Anillin during cytokinesis. *Semin Cell Dev Biol* 21 (9):881-91.
- Piekorz, R. P., A. Hoffmeyer, C. D. Dunsch, C. McKay, H. Nakajima, V. Sexl, L. Snyder, J. Rehg, and J. N. Ihle. 2002. The centrosomal protein TACC3 is essential for hematopoietic stem cell function and genetically interfaces with p53-regulated apoptosis. *EMBO J* 21 (4):653-64.
- Qin, G. W., and R. S. Xu. 1998. Recent advances on bioactive natural products from Chinese medicinal plants. *Med Res Rev* 18 (6):375-82.
- Qiu, C., et al. 2008. The studies on the anti-inflammatory and analgesia effects of SLW. *Pharmacology and Clinics of Chinese Materia Medica* 14:7-10.
- Reyes, H., S. Reisz-Porszasz, and O. Hankinson. 1992. Identification of the Ah receptor nuclear translocator protein (Arnt) as a component of the DNA binding form of the Ah receptor. *Science* 256 (5060):1193-5.

- Ribatti, D. 2008. Chick embryo chorioallantoic membrane as a useful tool to study angiogenesis. *Int Rev Cell Mol Biol* 270:181-224.
- Risau, W. 1997. Mechanisms of angiogenesis. *Nature* 386 (6626):671-4.
- Roy, A. M., K. N. Tiwari, W. B. Parker, J. A. Secrist, 3rd, R. Li, and Z. Qu. 2006. Antiangiogenic activity of 4'-thio-beta-D-arabinofuranosylcytosine. *Mol Cancer Ther* 5 (9):2218-24.
- Schmidt, J. V., and C. A. Bradfield. 1996. Ah receptor signaling pathways. *Annu Rev Cell Dev Biol* 12:55-89.
- Scoditti, E., N. Calabriso, M. Massaro, M. Pellegrino, C. Storelli, G. Martines, R. De Caterina, and M. A. Carluccio. 2012. Mediterranean diet polyphenols reduce inflammatory angiogenesis through MMP-9 and COX-2 inhibition in human vascular endothelial cells: a potentially protective mechanism in atherosclerotic vascular disease and cancer. *Arch Biochem Biophys* 527 (2):81-9.
- Sluimer, J. C., and M. J. Daemen. 2009. Novel concepts in atherogenesis: angiogenesis and hypoxia in atherosclerosis. *J Pathol* 218 (1):7-29.
- Sluimer, J. C., F. D. Kolodgie, A. P. Bijnens, K. Maxfield, E. Pacheco, B. Kutys, H. Duimel, P. M. Frederik, V. W. van Hinsbergh, R. Virmani, and M. J. Daemen. 2009. Thin-walled microvessels in human coronary atherosclerotic plaques show incomplete endothelial junctions relevance of compromised structural integrity for intraplaque microvascular leakage. *J Am Coll Cardiol* 53 (17):1517-27.
- Sridhar, S. S., and F. A. Shepherd. 2003. Targeting angiogenesis: a review of angiogenesis inhibitors in the treatment of lung cancer. *Lung Cancer* 42 Suppl 1:S81-91.
- Staton, C. A., M. W. Reed, and N. J. Brown. 2009. A critical analysis of current in vitro and in vivo angiogenesis assays. *Int. J. Exp. Pathol.* 90 (3):195-221.
- Suboj, P., S. Babykutty, D. R. Valiyaparambil Gopi, R. S. Nair, P. Srinivas, and S. Gopala. 2012. Aloe emodin inhibits colon cancer cell migration/angiogenesis by downregulating MMP-2/9, RhoB and VEGF via reduced DNA binding activity of NF-kappaB. *Eur J Pharm Sci* 45 (5):581-91.
- Sullivan, M., and D. O. Morgan. 2007. Finishing mitosis, one step at a time. *Nat. Rev. Mol. Cell Biol.* 8 (11):894-903.
- Sun, J., S. Wang, and Y. H. Wei. 2011. Reproductive toxicity of *Rhizoma Sparganii* (*Sparganium stoloniferum* Buch.-Ham.) in mice: mechanisms of anti-angiogenesis and anti-estrogen pharmacologic activities. *J Ethnopharmacol* 137 (3):1498-503.

- Swiercz, R., E. Skrzypczak-Jankun, M. M. Merrell, S. H. Selman, and J. Jankun. 1999. Angiostatic activity of synthetic inhibitors of urokinase type plasminogen activator. *Oncol Rep* 6 (3):523-6.
- Tassan, J. P., S. J. Schultz, J. Bartek, and E. A. Nigg. 1994. Cell cycle analysis of the activity, subcellular localization, and subunit composition of human CAK (CDK-activating kinase). *J. Cell Biol.* 127 (2):467-78.
- Ushio-Fukai, M., R. W. Alexander, M. Akers, Q. Yin, Y. Fujio, K. Walsh, and K. K. Griendling. 1999. Reactive oxygen species mediate the activation of Akt/protein kinase B by angiotensin II in vascular smooth muscle cells. *J Biol Chem* 274 (32):22699-704.
- van Royen, N., J. J. Piek, I. Buschmann, I. Hofer, M. Voskuil, and W. Schaper. 2001. Stimulation of arteriogenesis; a new concept for the treatment of arterial occlusive disease. *Cardiovasc Res* 49 (3):543-53.
- Vincent, L., W. Chen, L. Hong, F. Mirshahi, Z. Mishal, T. Mirshahi-Khorassani, J. P. Vannier, J. Soria, and C. Soria. 2001. Inhibition of endothelial cell migration by cerivastatin, an HMG-CoA reductase inhibitor: contribution to its anti-angiogenic effect. *FEBS Lett* 495 (3):159-66.
- Virmani, R., F. D. Kolodgie, A. P. Burke, A. V. Finn, H. K. Gold, T. N. Tulenko, S. P. Wrenn, and J. Narula. 2005. Atherosclerotic plaque progression and vulnerability to rupture: angiogenesis as a source of intraplaque hemorrhage. *Arterioscler Thromb Vasc Biol* 25 (10):2054-61.
- Wang, Q., L. Zou, W. Liu, W. Hao, S. Tashiro, S. Onodera, and T. Ikejima. Inhibiting NF-kappaB activation and ROS production are involved in the mechanism of silibinin's protection against D-galactose-induced senescence. *Pharmacol Biochem Behav* 98 (1):140-9.
- Wang, X. H., S. Y. Wu, and Y. S. Zhen. 2004. Inhibitory effects of emodin on angiogenesis. *Yao Xue Xue Bao* 39 (4):254-8.
- Wickstrom, S. A., K. Alitalo, and J. Keski-Oja. 2004. An endostatin-derived peptide interacts with integrins and regulates actin cytoskeleton and migration of endothelial cells. *J Biol Chem* 279 (19):20178-85.
- Wiesener, M. S., H. Turley, W. E. Allen, C. Willam, K. U. Eckardt, K. L. Talks, S. M. Wood, K. C. Gatter, A. L. Harris, C. W. Pugh, P. J. Ratcliffe, and P. H. Maxwell. 1998. Induction of endothelial PAS domain protein-1 by hypoxia: characterization and comparison with hypoxia-inducible factor-1alpha. *Blood* 92 (7):2260-8.
- Wu, H., R. Feng, S. Guan, W. Yu, W. Man, J. Guo, X. Liu, M. Yang, B. Jiang, W. Wu, L. Zhang, and D. Guo. 2012. Rapid preparative isolation of a new

- phenylpropanoid glycoside and four minor compounds from *Sparganium stoloniferum* using high-speed counter-current chromatography as a fractionation tool. *J Sep Sci* 35 (9):1160-6.
- Wu, Z., H. Cho, G. M. Hampton, and D. Theodorescu. 2009. Cdc6 and cyclin E2 are PTEN-regulated genes associated with human prostate cancer metastasis. *Neoplasia* 11 (1):66-76.
- Xiong, Y., K. Z. Deng, Y. Q. Guo, W. Y. Gao, and T. J. Zhang. 2009. New chemical constituents from the rhizomes of *Sparganium stoloniferum*. *Arch. Pharm. Res.* 32 (5):717-20.
- Yang, C., L. Czech, S. Gerboth, S. Kojima, G. Scita, and T. Svitkina. 2007. Novel roles of formin mDia2 in lamellipodia and filopodia formation in motile cells. *PLoS Biol* 5 (11):e317.
- Yang, H. S., D. M. Zhang, H. X. Deng, F. Peng, and Y. Q. Wei. 2010. Antitumor and anti-angiogenesis immunity induced by CR-SEREX-identified *Xenopus* RHAMM. *Cancer Sci* 101 (4):862-8.
- Zhou, L. G., and J. Y. Wu. 2006. Development and application of medicinal plant tissue cultures for production of drugs and herbal medicinals in China. *Nat Prod Rep* 23 (5):789-810.

APPENDIX A –SUPPLEMENTARY DATA

Table A.1 Gene function enrichment analysis for HUVECs in response to SsnB treatment

Gene Ontology					
C1	C2	C3	C4	P-value	Term Name
118	759	1470	15432	0	adenyl nucleotide binding
114	759	1386	15432	0	ATP binding
203	759	3326	15432	0.000397	cell communication
123	759	772	15432	0	cell cycle
15	759	75	15432	0.000007	cell cycle arrest
13	759	48	15432	0.000001	cell cycle checkpoint
64	759	258	15432	0	cell cycle phase
107	759	653	15432	0	cell cycle process
49	759	199	15432	0	cell division
54	759	588	15432	0.000013	cell proliferation
576	759	10922	15432	0.000936	cellular process
16	759	130	15432	0.000926	chemotaxis
38	759	286	15432	0	chromosomal part
44	759	337	15432	0	chromosome
13	759	43	15432	0	chromosome segregation
16	759	48	15432	0	chromosome, pericentric region
46	759	543	15432	0.000335	cytoskeletal part
66	759	897	15432	0.000881	cytoskeleton
47	759	439	15432	0.000001	cytoskeleton organization and biogenesis
17	759	119	15432	0.000121	cytoskeleton-dependent intracellular transport
57	759	711	15432	0.000271	DNA metabolic process
25	759	244	15432	0.000614	DNA repair
29	759	189	15432	0	DNA replication
16	759	96	15432	0.000033	DNA-dependent DNA replication
15	759	67	15432	0.000002	interphase
14	759	63	15432	0.000005	interphase of mitotic cell cycle
107	759	1541	15432	0.000199	intracellular non-membrane-bound organelle
66	759	897	15432	0.000881	kinase activity
57	759	214	15432	0	M phase
50	759	168	15432	0	M phase of mitotic cell cycle
25	759	202	15432	0.000037	microtubule
16	759	113	15432	0.000209	microtubule associated complex
37	759	290	15432	0	microtubule cytoskeleton

15	759	63	15432	0.000001	microtubule cytoskeleton organization and biogenesis
14	759	83	15432	0.000089	microtubule motor activity
17	759	105	15432	0.000027	microtubule-based movement
31	759	186	15432	0	microtubule-based process
48	759	166	15432	0	mitosis
58	759	226	15432	0	mitotic cell cycle
19	759	156	15432	0.000367	motor activity
75	759	873	15432	0.000003	negative regulation of biological process
71	759	806	15432	0.000002	negative regulation of cellular process
24	759	185	15432	0.000025	negative regulation of progression through cell cycle
107	759	1541	15432	0.000199	non-membrane-bound organelle
140	759	2090	15432	0.000093	nucleotide binding
14	759	91	15432	0.000225	phosphoinositide-mediated signaling
319	759	5058	15432	0	protein binding
134	759	1797	15432	0.000001	purine nucleotide binding
8	759	37	15432	0.000589	Ras GTPase activator activity
74	759	493	15432	0	regulation of cell cycle
217	759	3609	15432	0.000529	regulation of cellular process
9	759	41	15432	0.000245	regulation of cyclin-dependent protein kinase activity
14	759	46	15432	0	regulation of mitosis
74	759	490	15432	0	regulation of progression through cell cycle
31	759	282	15432	0.000042	response to DNA damage stimulus
31	759	304	15432	0.000157	response to endogenous stimulus
47	759	492	15432	0.000018	response to external stimulus
130	759	1996	15432	0.000545	response to stimulus
80	759	842	15432	0	response to stress
14	759	43	15432	0	spindle
16	759	130	15432	0.000926	taxis
76	759	1037	15432	0.000404	transferase activity, transferring phosphorus-containing groups
Protein Domain					
C1	C2	C3	C4	P-value	Term Name
4	542	9	12147	0.000781	AIG1 family // 9.1E-85
6	542	16	12147	0.000098	Cyclin, C-terminal // 4.0E-41
12	542	41	12147	0.000001	Kinesin, motor region // 4.1E-121
Pathway					
C1	C2	C3	C4	P-value	Term Name
31	180	112	2918	0	Cell_cycle_KEGG // GenMAPP
21	180	69	2918	0	DNA_replication_Reactome // GenMAPP
19	180	90	2918	0.000004	G1_to_S_cell_cycle_Reactome // GenMAPP
25	180	195	2918	0.000429	Smooth_muscle_contraction // GenMAPP

C1: number of genes in a cluster or list that have this annotation term

C2: number of annotated genes in this cluster or list

C3: number of all genes on array that have this annotation term

C4: number of all annotated genes on array

P-value: binomial approximated p-value for hypergeometric distribution

Table A.2 Gene function enrichment analysis for HCAECs in response to SsnB treatment

Gene Ontology					
C1	C2	C3	C4	P-value	Term Name
56	214	1470	15432	0	adenyl nucleotide binding
56	214	1386	15432	0	ATP binding
15	214	360	15432	0.000177	ATPase activity
13	214	311	15432	0.000463	ATPase activity, coupled
87	214	4602	15432	0.000477	biopolymer metabolic process
93	214	5029	15432	0.000574	catalytic activity
85	214	772	15432	0	cell cycle
13	214	48	15432	0	cell cycle checkpoint
51	214	258	15432	0	cell cycle phase
71	214	653	15432	0	cell cycle process
43	214	199	15432	0	cell division
27	214	588	15432	0	cell proliferation
51	214	2215	15432	0.000155	cellular component organization and biogenesis
179	214	10922	15432	0.000009	cellular process
32	214	286	15432	0	chromosomal part
35	214	337	15432	0	chromosome
19	214	377	15432	0.000002	chromosome organization and biogenesis
15	214	363	15432	0.000194	chromosome organization and biogenesis (sensu Eukaryota)
15	214	43	15432	0	chromosome segregation
18	214	48	15432	0	chromosome, pericentric region
6	214	34	15432	0.00001	condensed chromosome
30	214	543	15432	0	cytoskeletal part
31	214	897	15432	0.000003	cytoskeleton
28	214	439	15432	0	cytoskeleton organization and biogenesis
13	214	119	15432	0	cytoskeleton-dependent intracellular transport
4	214	30	15432	0.000877	DNA damage response, signal transduction
45	214	711	15432	0	DNA metabolic process
21	214	244	15432	0	DNA repair
30	214	189	15432	0	DNA replication
9	214	42	15432	0	DNA-dependent ATPase activity
18	214	96	15432	0	DNA-dependent DNA replication
4	214	26	15432	0.000517	double-stranded DNA binding
21	214	618	15432	0.000162	hydrolase activity, acting on acid anhydrides
21	214	615	15432	0.000152	hydrolase activity, acting on acid anhydrides, in phosphorus-containing anhydrides
12	214	67	15432	0	interphase
12	214	63	15432	0	interphase of mitotic cell cycle
140	214	7906	15432	0.000019	intracellular
108	214	5631	15432	0.000021	intracellular membrane-bound organelle
60	214	1541	15432	0	intracellular non-membrane-bound organelle
122	214	6494	15432	0.000008	intracellular organelle

62	214	2068	15432	0	intracellular organelle part
131	214	7364	15432	0.00005	intracellular part
47	214	214	15432	0	M phase
45	214	168	15432	0	M phase of mitotic cell cycle
108	214	5633	15432	0.000021	membrane-bound organelle
17	214	202	15432	0	microtubule
13	214	113	15432	0	microtubule associated complex
28	214	290	15432	0	microtubule cytoskeleton
12	214	63	15432	0	microtubule cytoskeleton organization and biogenesis
13	214	83	15432	0	microtubule motor activity
6	214	64	15432	0.000303	microtubule organizing center
13	214	105	15432	0	microtubule-based movement
25	214	186	15432	0	microtubule-based process
44	214	166	15432	0	mitosis
50	214	226	15432	0	mitotic cell cycle
13	214	156	15432	0	motor activity
60	214	1541	15432	0	non-membrane-bound organelle
21	214	583	15432	0.000073	nucleoside-triphosphatase activity
56	214	2090	15432	0.000001	nucleotide binding
101	214	3964	15432	0	nucleus
122	214	6495	15432	0.000008	organelle
44	214	1019	15432	0	organelle organization and biogenesis
62	214	2068	15432	0	organelle part
13	214	91	15432	0	phosphoinositide-mediated signaling
33	214	1302	15432	0.000564	post-translational protein modification
15	214	421	15432	0.000888	protein serine/threonine kinase activity
56	214	1797	15432	0	purine nucleotide binding
21	214	612	15432	0.000142	pyrophosphatase activity
43	214	493	15432	0	regulation of cell cycle
73	214	3609	15432	0.000246	regulation of cellular process
7	214	41	15432	0.000002	regulation of cyclin-dependent protein kinase activity
5	214	43	15432	0.00037	regulation of DNA metabolic process
13	214	46	15432	0	regulation of mitosis
43	214	490	15432	0	regulation of progression through cell cycle
24	214	282	15432	0	response to DNA damage stimulus
24	214	304	15432	0	response to endogenous stimulus
30	214	842	15432	0.000002	response to stress
13	214	219	15432	0.000015	second-messenger-mediated signaling
13	214	43	15432	0	spindle
28	214	1037	15432	0.00059	transferase activity, transferring phosphorus-containing groups
8	214	143	15432	0.000965	ubiquitin-protein ligase activity
Protein Domain					
C1	C2	C3	C4	P-value	Term Name
5	130	47	12147	0.000166	AAA ATPase, central region // 2.2E-18
4	130	29	12147	0.00029	BRCT // 9.8E-9

4	130	16	12147	0.00003	Cyclin, C-terminal // 4.0E-41
4	130	31	12147	0.000373	Cyclin, N-terminal domain // 3.6E-14
12	130	41	12147	0	Kinesin, motor region // 4.1E-121
2	130	4	12147	0.000884	Lysophospholipase, catalytic domain // 2.4E-63
2	130	3	12147	0.000501	M-phase inducer phosphatase // 1.7E-30
6	130	10	12147	0	MCM // 2.1E-66
2	130	4	12147	0.000884	SMC protein, N-terminal // 3.7E-50
Pathway					
C1	C2	C3	C4	P-value	Term Name
27	60	112	2918	0	Cell_cycle_KEGG // GenMAPP
22	60	69	2918	0	DNA_replication_Reactome // GenMAPP
16	60	90	2918	0	G1_to_S_cell_cycle_Reactome // GenMAPP

C1: number of genes in a cluster or list that have this annotation term

C2: number of annotated genes in this cluster or list

C3: number of all genes on array that have this annotation term

C4: number of all annotated genes on array

P-value: binomial approximated p-value for hypergeometric distribution

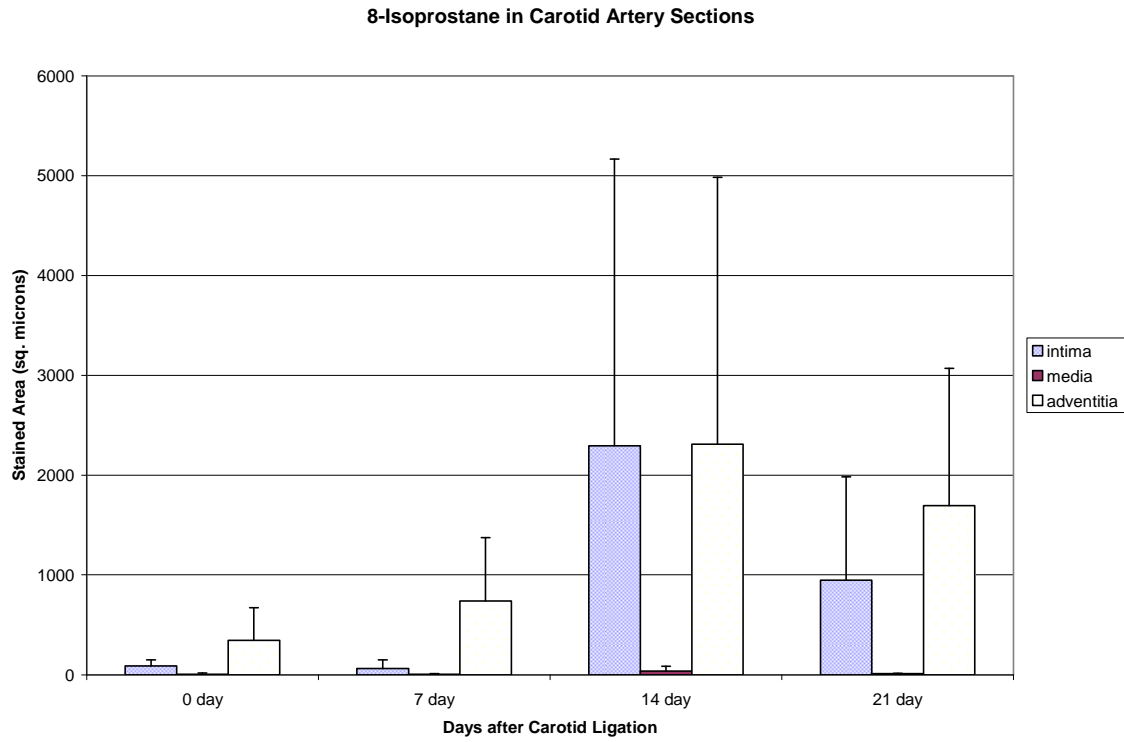


Figure A.1 8-Isoprostane Staining in Sections of Carotid Arteries

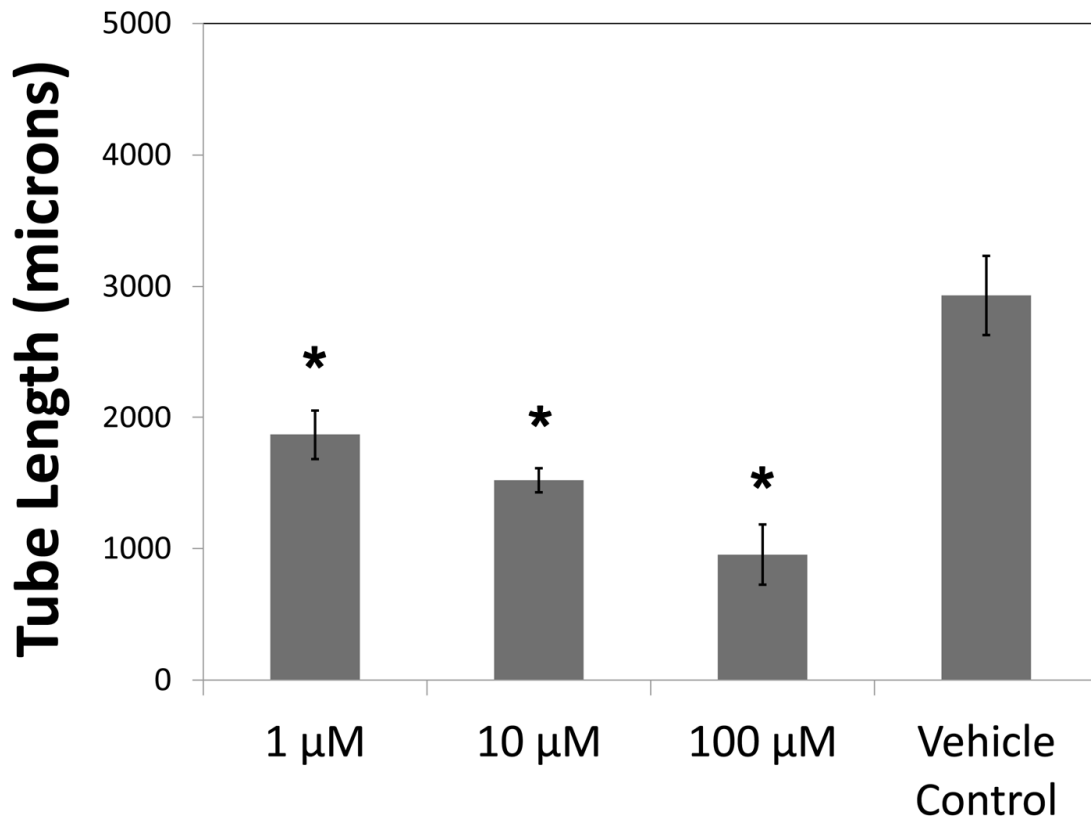


Figure A.2 SsnB inhibits Matrigel tube formation in HMVECs

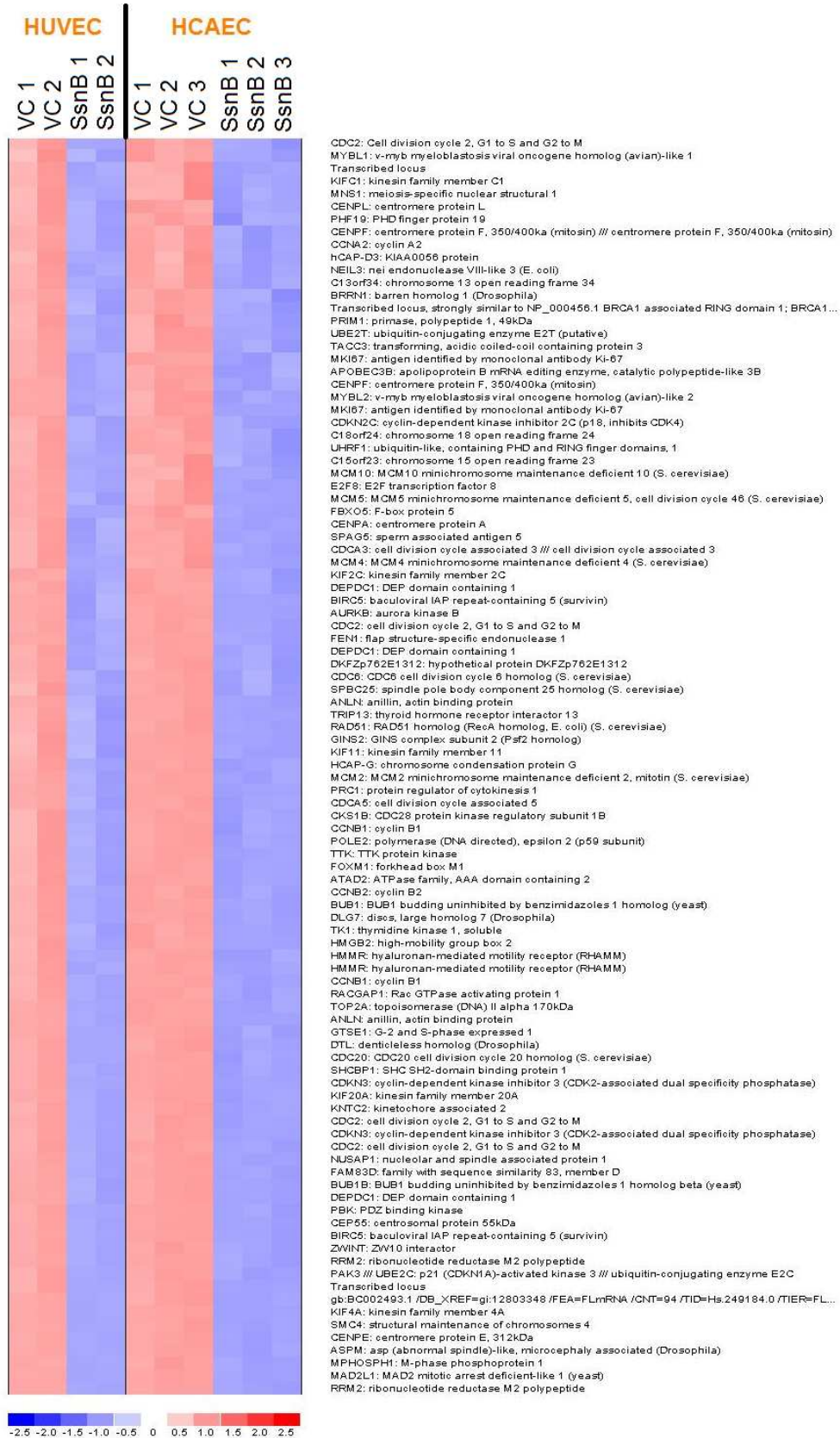


Figure A.3 Heatmap of differentially regulated genes in HUVECs and HCAECs

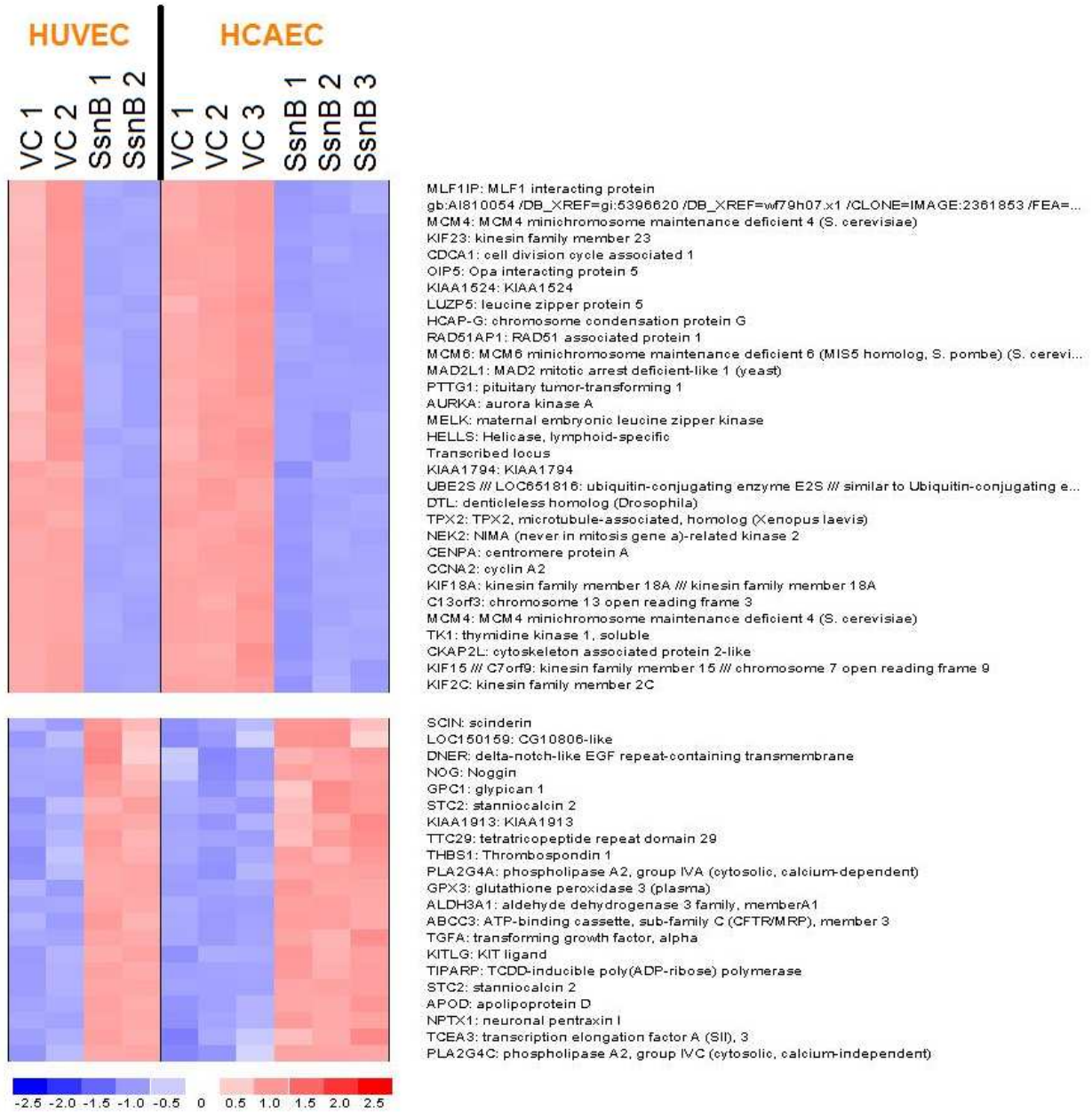


Figure A.4 Heatmap of differentially regulated genes in HUVECs and HCAECs

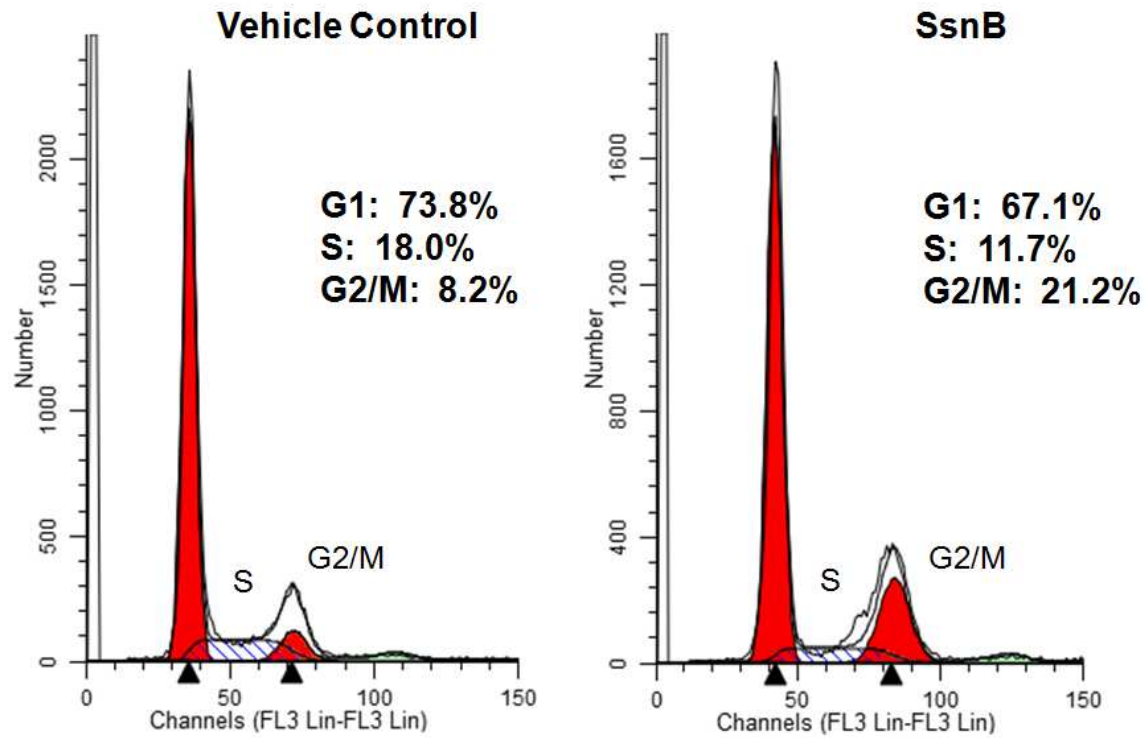


Figure A.5 SsnB causes G2/M blockage in non-synchronized HUVECs

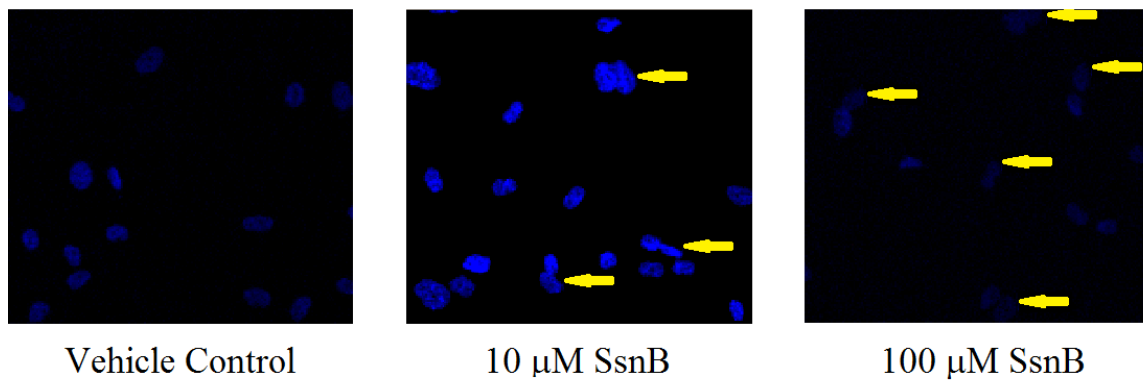


Figure A.6 Representative images demonstrating double nuclei (indicated by arrows)